Journal of Hydrology 655 (2025) 132896

Contents lists available at ScienceDirect

Journal of Hydrology

journal homepage: www.elsevier.com/locate/jhydrol

Research papers

Local- and global-scale hydrological and sediment connectivity over grassland and shrubland hillslopes

Shubham Tiwari *, Laura Turnbull, John Wainwright

Department of Geography, Durham University, Durham, United Kingdom

ARTICLE INFO

This manuscript was handled by S Sally Elizabeth Thompson, Editor-in-Chief, with the assistance of Giulia Vico, Associate Editor

Keywords:
Emergent patterns
Functional connectivity
Structural connectivity
Network theory
Land degradation
Grass-shrub transition

ABSTRACT

Quantifying connectivity patterns in dryland ecosystems enables us to understand how changes in the vegetation structure influence the runoff and erosion processes. This knowledge is crucial for mitigating the impacts of climate change and land use modifications. We quantify the multi-scale water-mediated connectivity within grassland and shrubland hillslopes using a weighted, directed network model. By integrating high-resolution elevation data, vegetation information, and modeled event-based hydrologic and sediment transport, we assess both structural connectivity (physical landscape layout) and functional connectivity (dynamic water and sediment movement) under varying rainfall and soil moisture conditions.

Our findings reveal a marked increase in local (patch-scale) connectivity metrics in shrublands compared to grasslands. Metrics like betweenness centrality—which measures the importance of nodes in connecting different parts of the network—and the weighted length of connected pathways increase up to tenfold in shrublands. Despite substantial local changes, global (plot-scale) properties like efficiency of water and sediment transfer show less variation, suggesting a robust network topology that sustains geomorphic functionality across different vegetation states.

We also find that the functional connectivity is more strongly correlated with structural connectivity for sediment than for water. This difference is particularly pronounced under high rainfall conditions and shows little sensitivity to variations in antecedent soil moisture, highlighting the critical role of rainfall-driven processes in shaping connectivity patterns.

The study offers a comprehensive framework for analyzing connectivity at multiple scales, which can inform targeted management strategies aimed at enhancing ecosystem resilience, such as interventions to control erosion or restore vegetation patterns.

1. Introduction

Drylands, defined as regions with an aridity index less than 0.65, cover approximately 41.3 % of the global land surface (Prăvălie, 2016; Reynolds et al., 2007). These ecosystems provide vital ecological services despite harsh environmental conditions characterized by low rainfall, high evapotranspiration, and extreme temperature variability (Noy-Meir, 1973; Reynolds et al., 2007). Drylands have unique biodiversity (Maestre et al., 2016a, Maestre et al., 2021), store over 30 % of terrestrial carbon stocks (Cunliffe et al., 2016; Lal, 2019), and support 38 % of the global population (United Nations, 2022). Therefore, understanding the drivers of dryland landscape structure and functional dynamics is both an urgent scientific concern and a pressing societal need.

Landscape structure refers to the physical layout of the landscape, such as vegetation patterns, and topography, which affect how resources (water and sediment in the context of this study) are distributed (Tiwari et al., 2024; Turnbull et al., 2008). Function describes the dynamic processes, like water flow and sediment transport, that depend on these structural features (Tiwari et al., 2024; Turnbull et al., 2008).

The structure and functional dynamics of drylands are significantly influenced by connectivity — the physical linkage that facilitates the flow of water and sediment across the landscape (Reynolds et al., 2007; Turnbull et al., 2008). This connectivity is crucial for the redistribution of resources, impacting biodiversity and ecosystem services including forage provision, soil retention, and carbon storage (Bestelmeyer et al., 2011; Maestre et al., 2016b; Schlesinger et al., 1990). In these landscapes, vegetation structure exerts strong controls on the connectivity of

* Corresponding author.
E-mail address: shubham.tiwari@durham.ac.uk (S. Tiwari).

https://doi.org/10.1016/j.jhydrol.2025.132896
Received 22 July 2024; Received in revised form 10 December 2024; Accepted 2 February 2025
Available online 26 February 2025

water and sediment transfers across the landscape (Bestelmeyer et al., 2018; Calvo-Cases et al., 2021; Meron, 2018; Okin et al., 2015; Turnbull et al., 2012; Wainwright et al., 2011).

In many drylands, grassland and shrubland represent alternative vegetation states across aridity gradients (Maestre et al., 2016a; Okin et al., 2009; Peters et al., 2020, 2006; Pierce et al., 2019; Romero Ovalle et al., 2021; Turnbull and Wainwright, 2019). Transitions between grassland and shrubland are principally thought to be driven by drought, grazing and fire (Okin et al., 2009). These drivers change the local structure of vegetation and soil-surface properties, subsequently altering hydrologic and sediment transport connectivity during rainfall events (Bestelmeyer et al., 2018; Okin et al., 2009; Turnbull et al., 2012). At shorter temporal scales, changes occur during rainfall events due to immediate shifts in surface flows, while at longer temporal scales, the impacts of vegetation and soil modifications emerge more gradually. These changes in vegetation structure can trigger feedback mechanisms that either enhance or degrade landscape resilience to future shifts, depending on how they impact redistributive flows and fluxes (Scheffer and Carpenter, 2003; Turnbull et al., 2008). Resilience, in this context, refers to the ability of a landscape to absorb disturbances (such as increase in land-use pressures or climatic variability) while maintaining its functional integrity, including the capacity to sustain hydrological and sedimentary processes essential for ecosystem stability (Folke, 2006; Holling, 1973). A resilient landscape can adapt to changes and recover from perturbations without transitioning to an alternative state, such as from grassland to shrubland or vice versa, while ensuring the continued redistribution and retention of critical resources like water, and sediments (Jenerette et al., 2012; Price, 2003; Turnbull et al., 2008).

Connectivity-driven stabilizing feedbacks maintain existing patch structures and functions, such as resource retention in grasslands (Abrahams and Parsons, 1996; Parsons et al., 1996; Schlesinger et al., 1990; Turnbull et al., 2008). Alternatively, amplifying feedbacks progressively diminish resilience and facilitate state changes. A classic example is shrub encroachment reducing infiltration, elevating runoff, and increasing erosion (Peters et al., 2006; Schlesinger et al., 1990). These positive feedbacks favour and drive further shrub expansion.

Despite the recognized importance of connectivity in shaping dryland ecosystems (Bestelmeyer et al., 2011; Okin et al., 2009; Peters et al., 2006; Tiwari et al., 2024; Turnbull et al., 2008; Turnbull and Wainwright, 2019), barriers to its quantification exist. A primary challenge is translating conceptual models of connectivity into quantitative metrics that accurately represent the complex processes and interactions involved (Okin et al., 2009). Common approaches in geomorphology, such as the Index of Connectivity (Borselli et al., 2008; Cavalli et al., 2013) focus on structural connectivity, and not on the dynamical/functional aspects of connectivity (FC) that vary over time. Other approaches that have lookde at both structural and functional aspects of connectivity oversimplify connectivity by reducing it to a binary presence/absence of pathways (e.g. Bracken et al., 2015; Turnbull and Wainwright, 2019; Wohl et al., 2019), thereby obscuring the spatial dynamics of flow and resulting variations in the strength of connections (Barrat et al., 2004).

Connectivity can be quantified at two distinct scales: the scale of patch (referred to as the local scale) and the scale of the entire plot (referred to as the global scale). Local connectivity metrics quantify the interactions and linkages between neighboring landscape elements (e.g., patches), reflecting small-scale processes such as the redistribution of water or sediment across adjacent areas. Global connectivity metrics encompass the overall network structure and describes the large-scale patterns of resource transfer or flow across the entire system.

Work to date has emphasized the usefulness of metrics that quantify the length or density of connected pathways (e.g. Okin et al. 2009, Stewart et al. 2014, Turnbull and Wainwright 2019). However, these measures often fail to capture other important aspects of connectivity, such as the strength and directionality of resource flows, especially at multiple scales. There is untapped potential in applying network metrics that can quantify both local and global-scale emergent patterns of connectivity (Tiwari et al., 2024), providing a more comprehensive understanding of geomorphic systems. The novelty of our work lies in applying advanced network-based approaches, specifically weighted and directed networks, to quantify connectivity patterns in dryland hillslopes. In these networks, the landscape is modeled as a set of nodes (e.g., landscape patches or grid cells) connected by links that have both direction and weight, capturing the magnitude and flow direction of resources like water or sediment (Tiwari et al., 2024). The utility of network-based approaches for improving understanding of connectivity in deltas and estuaries already been demonstrated (Hiatt et al., 2022, 2018; Passalacqua, 2017; Tejedor et al., 2015) and there is clearly great potential for network-based approaches to improve our quantitative understanding of hillslope connectivity. Work already undertaken in this area includes the exploration of overland flow connectivity on semi-arid hillslopes (Calvo-Cases et al., 2021) and sediment cascades in alpine catchments (Cossart and Fressard, 2017; Heckmann and Schwanghart, 2013). Tiwari et al., (2024) explored how hillslopes can be represented as weighted and directed networks to allow robust quantification of connectivity patterns. They used tools and metrics from complex network theory, such as degree centrality, betweenness centrality, and global efficiency (which are used in this study and defined later in Section 2), and demonstrated that weighted-directional networks can capture the strength and directionality of water and sediment flows.

Translating these developments in networks to hillslope geomorphology, we can model water-mediated connectivity over a hillslope as a network where nodes represents specific locations or patches (e.g. areas of different vegetation cover) and links, where links represent the pathways of water or sediment flow between them, weighted by factors such as flow magnitude or sediment load. Structural Connectivity (SC) in this study describes the static spatial arrangement and potential connections based on landscape features like microtopography and vegetation (Maestre et al., 2016a; Turnbull and Wainwright, 2019). Functional Connectivity (FC), on the other hand, characterizes the dynamic and actual movement of water and sediment over the SC, influenced by factors like rainfall events and soil moisture (see Tiwari et al., 2024; Turnbull et al., 2018 for a further discussion of issues concerning the separation of structural and functional connectivity in geomorphology).

Understanding how SC influences FC is crucial for grasping how landscape structure affects water and sediment movement, and the potential for FC-SC feedbacks over longer timescales. By quantifying both SC and FC, we can investigate the relationship between them (see Voutsa et al, 2021 for a discussion of SC-FC relations in geomorphology, and other disciplines). Specifically, we can quantify how differences in network topology (SC) give rise to distinct and diverse patterns of FC, and under what circumstances. The nature of the SC-FC relation may vary depending on the system and process, with SC exerting a stronger or weaker influence on FC.

Previous work has explored where and when there are similarities in the length of connected pathways between SC and FC on dryland hillslopes, suggesting the potential for feedbacks between structure and function (e.g. Turnbull and Wainwright, 2019). Building on this foundation, there is a scope to explore a wider suite of SC-FC relations by utilizing various connectivity metrics. These metrics can provide insights into different aspects of hillslope-scale hydrological and sediment connectivity. In particular, quantitatively assessing where and when there are similarities/differences in hydrological and sediment connectivity can enhance our understanding of these systems.

In this study, we focus on grassland and shrubland hillslopes in New Mexico, USA—a region representative of grass-shrub transitions commonly found in dryland ecosystems across the southwestern United States. We aim to understand how differences in landscape structure between grassland and shrubland hillslopes influence hydrological and sediment connectivity. To achieve this, we focus on the following specific research questions:

1. How do the global and local-scale characteristics of structural connectivity differ between grassland and shrubland hillslopes?
2. How do these differences in structural connectivity affect the functional connectivity of water (FC_{hyd}) and sediment (FC_{sed}) under varying environmental conditions, such as different rainfall events and antecedent soil moisture levels?
3. What is the nature of the relation between structural and functional connectivity in these ecosystems, and how does it vary between grassland and shrubland states? Specifically, does structural connectivity exert a stronger or weaker influence on functional connectivity for water versus sediment connectivity?

To answer these questions, we first determine how the global and local-scale characteristics of SC and FC vary between grassland and shrubland hillslopes. Then, we explore the types and strengths of the relations between SC and FC in these ecosystems.

2. Materials and methods

2.1. Study area

The drylands of the US Southwest contain a mosaic of grassland and shrubland ecosystems. Widespread shrub encroachment into native grasslands has been documented across this region (Gao and Reynolds, 2003; Van Auken, 2000). The network-based connectivity analysis developed here builds upon extensive work undertaken over grassland and shrubland hillslopes at the Sevilleta Long Term Ecological Research (LTER) site in central New Mexico (Turnbull et al., 2008, 2010a, 2010b, 2012; Turnbull and Wainwright, 2019), which are representative end-members of Chihuahuan desert grassland and shrubland states. These hillslopes have contrasting soil and vegetation characteristics (Turnbull et al., 2010c), summarized in Table 1. The justification for focussing on these well-studied hillslopes is that there is detailed information readily available that allows for detailed characterization of SC and FC networks. The Sevilleta has a semi-arid climate with a mean annual precipitation of 256 mm, 55 % arriving in the summer monsoon season (July-September), and a mean annual temperature of 13.2 °C (Collins et al. 2020).

2.2. Structural and functional connectivity networks

To develop SC and FC networks, it is necessary to establish (1) the fundamental unit of connectivity that is appropriate for the system in question; in other words, what does a node within a network represent, and (2) how to define links between these nodes that represent SC and FC (Tiwari et al., 2024; Turnbull et al., 2018). At the hillslope scale, hydrologically and geomorphologically relevant fundamental units can be defined based on vegetation patch patterns and their associated microtopography. In practice, the choice of suitable fundamental unit is often constrained by the spatial resolution of available data (e.g. elevation data, vegetation data), or, where models are used to simulate dynamical processes, the spatial resolution of the model outputs (Tiwari et al., 2024; Turnbull et al., 2018).

In this study, the focus of analysis is event-based hydrological and sediment connectivity, i.e. connected resource flows that occur during single rainfall-runoff events. At this timescale, SC is considered to be static, whereas FC is dynamic, and will likely vary in response to the SC of the landscape, rainfall characteristics and antecedent conditions.

We develop the SC network based on the way surface characteristics (topography and vegetation cover) are structured to create pathways that are a conduit for the connected transfer of water and sediment (Fig. 1) (i.e. network topology). Nodes represent landscape patches on a lattice grid, each with associated vegetation cover and elevation data. Edges between nodes are determined based on the D4 steepest descent flow routing.

The vegetation patterns were digitized from high-resolution aerial imagery and validated using field surveys. Percent vegetation cover for each node was calculated based on the proportion of vegetated area within the corresponding pixel or grid cell (Turnbull et al., 2010a). For upslope nodes, vegetation cover values were directly extracted for each node in the lattice. We only considered nodes to be connected if the vegetation of the upslope node was less than or equal to 60 % cover (Turnbull and Wainwright, 2019). The rationale for vegetation-related connectivity/disconnectivity in the SC network is based on previous research showing that vegetation patches facilitate run-on infiltration, leading to resource retention and disconnected flows (e.g. Wainwright et al. 2002, Abrahams et al. 2003). A vegetation cover value of 60 % was used as this threshold is informed by percolation theory, which describes how connectivity in a system emerges based on the proportion of occupied sites (Stauffer and Aharony, 2018). In two-dimensional lattices with four nearest neighbors (analogous to our grid), the critical percolation threshold—the point at which a system transitions from being predominantly disconnected to connected—occurs around 59 % for finite systems is the midpoint in the range of observed percolation thresholds for finite lattices with 4-coordination in two-dimensional systems (Harel and Mouche, 2014). Applying this concept to ecohydrological processes, the percolation threshold represents the critical point where the landscape shifts from facilitating overland flow (and thus resource transfer) to inhibiting it due to increased vegetation cover. By selecting 60 % as the threshold, we capture this critical transition, reflecting the ecohydrological tipping point at which increased vegetation cover markedly diminishes the potential for surface runoff and resource transfer downslope.

Link weight in the SC network is inversely proportional to the vegetation cover of the source node; specifically, it is equal to the normalized value of the difference between the maximum percentage vegetation cover of a node that can be structurally connected to downslope nodes (i.e., 60 %) and the percentage vegetation cover of the source node. For example, if a source node has a 10 % vegetation cover, then the weight associated with the link originating from it will be (60–10)/60, i.e., 5/6. In addition, nodes with vegetation cover ≥60 % have no links originating from them, i.e., 0 link weight. This inverse relation reflects the ecohydrological process where lower vegetation cover leads to higher potential for overland flow and sediment transport downslope, while higher vegetation cover reduces this potential by enhancing infiltration and acting as a barrier to flow. In this characterization of SC, denser vegetation produces weaker SC links to downslope nodes, to reflect the control of intercepting vegetation on reducing the potential for resource transfer. Whilst we focus on vegetation cover as the only factor influencing SC link weights, other factors such as

Table 1
Summary of vegetation and soil characteristics for grassland and shrubland plots. (Turnbull et al., 2010b). Vegetation cover represents the average proportion of each plot area covered by any live vegetation (grass or shrubs) based on digitized aerial imagery and field measurements. Soil characteristics represent plot-level averages from field-sampled and laboratory-analysed data (Turnbull et al., 2010b).

Plot	Vegetation Characteristics			Soil Characteristics			
Each plot measures 30 m × 10 m with an average slope of approximately 5 %.	% Vegetation Cover	% Grass Cover	% Shrub Cover	% Pebbles	% Sand	% Silt	% Clay
Grassland	45.5	45.5	0	27.8	50.8	18.8	2.6
Shrubland	23.3	1	22.3	34.0	43.8	20.0	2.2

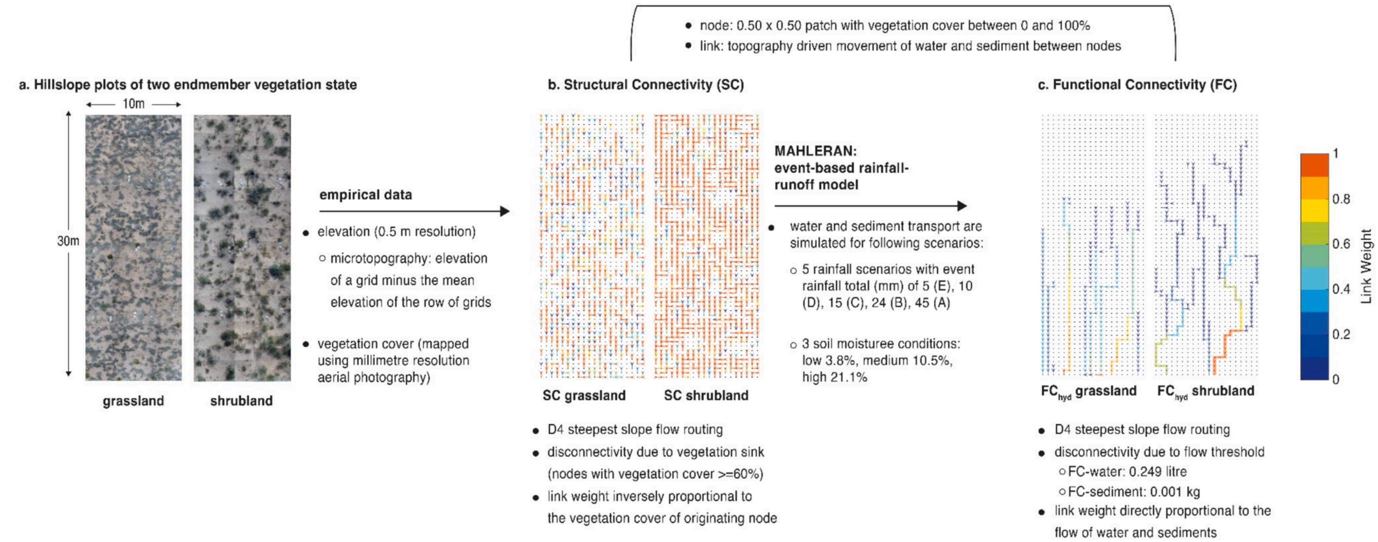

Fig. 1. (a) Aerial image showing grassland and shrubland hillslope plots. (b) Structural Connectivity (SC) network conceptualized using the D4 steepest slope algorithm and incorporating the disconnectivity caused by vegetation sinks i.e. nodes with vegetation cover more than 60 percent. (c) Functional Connectivity (FC) network constructed using the D4 steepest slope algorithm and incorporating the disconnectivity due to low flow/no flow conditions. The FC_{hyd} networks presented in this figure were generated from spatial simulations of runoff using MAHLERAN, under 45 mm total rainfall, and a mean antecedent soil-moisture content of 21 %.

slope, surface roughness, and downslope distance could also play a role in determining the strength of these connections (Tiwari et al., 2024).

The FC network for grassland and shrubland hillslopes was generated using spatially explicit, event-based runoff and sediment transport simulations presented and validated in Turnbull et al. (2010a, 2010b, 2010c), Turnbull and Wainwright (2019). These simulationswere performed using MAHLERAN (Model for Assessing Hillslope-Landscape Erosion, Runoff, and Nutrients), an event-based runoff and erosion model (Wainwright et al. 2008a, 2008b, 2008c). MAHLERAN simulates key hydrological and sediment transport processes, including runoff generation, flow routing (kinematic wave approximation), runon infiltration, splash erosion, and flow-driven sediment transport. Sediment is either transported downslope or deposited in areas of reduced flow energy (Wainwright et al., 2008a).

MAHLERAN has been extensively validated across a wide range of dryland environments, including semi-arid grassland and shrubland transitions, and has been shown to reliably simulate realistic runoff and sediment transport dynamics (Mueller, 2014; Turnbull et al., 2010a; Turnbull and Wainwright, 2019; Wainwright et al., 2008c). Validation efforts include comparisons of model output with measured hydrographs, sediment yield, and particulate nutrient fluxes under natural rainfall conditions at the Sevilleta Long-Term Ecological Research (LTER) site in New Mexico, USA (Turnbull et al., 2010a; Wainwright et al., 2008c). These validations included tests of runoff at the plot outlet, sediment yields, and spatial patterns of connectivity derived from monitored flow paths (Turnbull et al., 2010a). The agreement between modelled and monitored runoff, erosion, and nutrient transport dynamics demonstrates the robustness of MAHLERAN for capturing hydrological and sediment transport processes.

For this study, the spatially gridded model outputs (discharge and sediment transport) are converted to directed FC networks for water (FC_{hyd}) and sediment (FC_{sed}). We use the Deterministic 4-neighbor (D4) steepest descent flow routing to determine the connections between nodes, consistent with the approach used for the SC networks. Because the FC_{hyd} and FC_{sed} networks are created using modelled data, in which infinitely small hydrological and sediment fluxes can be quantified, we determined if two nodes were functionally connected if the modelled flux at each grid cell exceeded a threshold amount that would be observable under field conditions, set to 0.8 mm flow depth, as per Turnbull & Wainwright, (2019), and 1 g sediment which is the lowest steady-state value on similar plots for splash erosion (Parsons et al. 1994). Links in the FC_{hyd} and FC_{sed} networks were weighted by the flux normalized by the maximum simulated fluxes of all the simulations (3.86 l for water and 14 g for sediment transport). This normalisation enabled the comparison of FC_{hyd} and FC_{sed} networks across both vegetation types and environmental conditions (see Fig. 1 for a summary of methods).

The FC_{hyd} and FC_{sed} networks were constructed for different antecedent soil-moisture conditions (low, 3.8 %; medium, 10.5 %; high, 21.1 %) and for different rainfall events with total event rainfall of 45 mm, 24 mm, 15 mm, 10 mm and 5 mm which were selected based on analysis of the long-term rainfall record at the Sevilleta National Wildlife Refuge (as presented in Turnbull and Wainwright 2019). For each rainfall event, simulations were performed under all three antecedent soil-moisture conditions to evaluate how varying initial soil moisture influenced functional connectivity for both water (FC_{hyd}) and sediment (FC_{sed}).

2.3. Quantification of the connectivity patterns

2.3.1. Global-level metrics

Global-level metrics (i..e metrics characterising the whole network) are useful for understanding how connectivity between individual nodes leads to global network characteristics (i.e. a landscape-scale quantification of SC and FC). Here, we use three network-level metrics – Centralization Degree, Assortative Coefficient, and Global Efficiency – chosen for their relevance to landscape-scale processes as presented in Table 2 and explored in Tiwari et al. (2024).

Centralization Degree (CD) quantifies how centralized connectivity is within a network and is calculated by summing the differences between the maximum degree centrality and each node's degree, normalized by the maximum possible sum of differences (Equation (1),

$$CD = \frac{\sum_{i=1}^{N}(\max(S) - S_i)}{(N-1)(N-2)} \tag{1}$$

where S_i is the strength of node i, i.e. the sum of total link weights connected to a node (both incoming and outgoing) and N is the total number of possible links. Conventionally, networks with high degree centralization tend to have connectivity consolidated through a few focal nodes, making them more vulnerable to disruptions at those key

Table 2
Summary of global- and node-level network metrics, their descriptions, and corresponding equations for analyzing structural and functional connectivity.

Metric	Abbreviation	Description	Relation to Resilience	Equation Reference
Centralization Degree (Freeman, 1978)	CD	Measures how centralized connectivity is within a network. High CD indicates connectivity is concentrated through a few key nodes, making these nodes critical for overall system function.	High CD can reduce resilience because the system becomes more vulnerable to disruptions at key nodes. Conversely, low CD implies a more decentralized network, enhancing resilience by distributing resource flows and reducing dependency on specific nodes.	Equation (1)
Global Efficiency (Latora and Marchiori, 2001)	GE	Represents the network's ability to maintain connectivity, even when local connections are disrupted. Higher GE implies a more resilient network with efficient resource redistribution.	High GE enhances resilience of network connectivity by enabling efficient resource redistribution even when parts of the network are disrupted. A network with high GE can better withstand and recover from disturbances, maintaining overall functionality.	Equation (2)
Assortativity Coefficient (Newman, 2002)	AC	Quantifies the tendency of nodes to connect with others having similar (or dissimilar) traits. Positive AC indicates similar-node connections; negative AC indicates connections between dissimilar nodes.	Positive AC can enhance resilience by promoting uniform resource distribution and reducing erosion hotspots. Negative AC may reduce resilience by creating concentrated flows and increasing vulnerability to disturbances. Understanding AC helps in managing trait distributions to bolster resilience.	Equation (3)
Weighted Length of Connected Pathways (Okin et al., 2009)	WLOCOP	Measures the weighted length of connected pathways reaching a node, highlighting its role in long-distance resource redistribution.	Nodes with high WLOCOP are crucial for maintaining long-range connectivity. Their presence enhances resilience by ensuring that resources can be transferred across the landscape. Their loss can significantly reduce connectivity, making the system more susceptible to disturbances.	Equation (4)
Betweenness Centrality (Girvan and Newman, 2002; Tiwari et al., 2020)	BC	Reflects a node's importance as a connector within the network by counting the number of shortest paths that pass through it. High BC nodes act as critical conduits for resource flow.	High BC nodes are essential for network integrity and resilience. Their disruption can fragment the network, reducing overall connectivity. Identifying and protecting high BC nodes can enhance resilience by maintaining critical pathways for resource flow.	Equation (5)
Relative Node Efficiency (Crucitti et al., 2006)	RNE	Evaluates the impact of a node's removal on global connectivity. Positive RNE indicates that removal decreases network connectivity, while negative RNE suggests an increase in global efficiency due to the removal of redundant or inefficient nodes.	Understanding RNE helps identify nodes that are critical for resilience. Protecting nodes with positive RNE can maintain or enhance network robustness. Conversely, modifying or removing nodes with negative RNE can improve network efficiency and resilience by eliminating bottlenecks or redundant pathways.	Equation (6)

locations. In the context of this study, a high CD suggests that indicates that the movement and redistribution of water and sediment are disproportionately routed through a few critical nodes or pathways, which often correspond to areas of more concentrated flow, potentially leading to increased runoff, erosion, and the loss of dissolved and particle-bound resources such as carbon, nitrogen, and phosphorus (Parsons et al., 1994; Schlesinger et al., 1990). These areas are vital for the system's functioning because they facilitate efficient resource transfer. However, such centralization can reduce the resilience of the landscape by creating dependencies on these key pathways. If these pathways are disrupted—such as through revegetation efforts aimed at reducing structural connectivity—the flow patterns may shift, potentially decreasing erosion and enhancing resource retention by promoting infiltration and vegetation-mediated redistribution.

Global Efficiency (*GE*) is a measure of how efficiently resources are transferred across the network and inversely related to topological distance between nodes (Equation (2):

$$GE = \sum_{i=1}^{n} \sum_{j=1, i\neq j}^{n} \frac{1}{w_{ij} \times d_{ij}} \tag{2}$$

where d_{ij} is the shortest path length distance between node pair *i* and *j*, and w_{ij} is the mean weight of the path between *i* and *j*. For unweighted network, w_{ij} is equal to 1. A higher GE indicates a more globally connected and efficient network, where resources can be transferred quickly and through multiple pathways.

In terms of resilience, a network with high GE is considered more robust because it can efficiently reroute flows in response to localized disturbances, thereby maintaining overall functionality (Zhang and Ng, 2021). In dryland landscapes, higher GE implies that the system can better withstand changes such as vegetation loss or erosion because alternative pathways exist for resource redistribution. Conversely, a network with low GE may be more vulnerable to disruptions, as resources have fewer pathways and longer distances to traverse, potentially leading to localized degradation.

Complex networks often exhibit "assortative mixing," where highly connected nodes tend to link to other highly connected nodes (and low to low) (Newman, 2002). The Assortativity Coefficient (AC) quantifies the tendency of nodes to connect with other nodes having similar (assortative mixing) or dissimilar (disassortative mixing) traits Equation (3):

$$AC(x) = r(x_i, x_j) \tag{3}$$

where r is the Pearson correlation coefficient between the trait values x_i and x_j for all connected node pairs i and j. In directed networks, weconsider the correlation between the traits of nodes with outgoing links (x_i) andincoming links (x_j). This approach captures the directional mixing patterns across the network. As AC calculations only depend on the nodes' traits, it is unaffected by link weights.

In our context, we apply AC to vegetation cover and microtopography to determine whether hydrological and sediment connectivity links nodes with similar vegetation density and microtopography (assortativity) or connects different vegetation density and microtopography (disassortativity). Positive AC values indicate that nodes tend to connect with others having similar vegetation density or microtopography. Negative values suggest that nodes connect with dissimilar nodes (Boccaletti et al., 2006).

The microtopography of each node is calculated based on the elevation of the node minus the mean elevation of its neighbouring nodes, allowing for approximate analysis of the landscape's fine-scale relief. By analyzing AC, we can infer how the distribution of vegetation AC (vegetation) and AC (microtopogtaphy) influences connectivity patterns and resilience. For instance, assortative networks may be more stable and resilient to disturbances because similar nodes support each other, while disassortative networks may be more susceptible to cascading failures due to the dependence of nodes on dissimilar others.

In the results section, we present global metrics for the entire hillslope plots as well as for three spatial areas: up-slope, mid-slope, and down-slope regions. This approach allows for a more detailed understanding of how connectivity patterns vary across different parts of the hillslope. By comparing global metrics for these spatial areas, we can identify potential differences in regional connectivity characteristics (i.e. as a mid-level between global and node-level characteristics) and their implications for resource redistribution within the landscape.

2.3.2. Node-level metrics

Node-level metrics provide information about the role of a node in supporting connected pathways (Table 2). Here, we quantify node importance using Length of Connected Pathways Weighted (WLOCOP), Betweenness Centrality (BC), and Relative Node Efficiency (RNE), to allow greater insight into the role of individual landscape patches on system connectivity and resilience.

Previous studies in drylands have used the length of flow pathways as a way to quantify hydrological connectivity (Mayor et al., 2019, 2013; Turnbull and Wainwright, 2019). Okin et al. (2009) used the Length of Connected (incoming) Pathways (LOCOP) to demonstrate the role of vegetation cover in propagating dryland connectivity driven by water, wind, and fire. Their conceptual model provided insights on how different resource transport vectors interact with vegetation types to influence connectivity. Here we extend this concept to a quantitative network metric, Weighted Length of Connected (incoming) Pathways (WLOCOP), that considers edge weights. The WLOCOP thus builds upon the LOCOP conceptual framework, providing a measurable index of the extent to which a node, u, is directly connected to upslope regions, as modified by edge weight Equation (4).

$$WLOCOP_u = \sum_{i,j} l_{ij} \times w_{ij} \tag{4}$$

where l_{ij} is the mean length and w_{ij} is the mean weight of all the incoming pathways to node u (w_{ij} is equal to 1 for unweighted network). Nodes with high WLOCOP are crucial for maintaining connectivity over larger spatial scales, thus contributing to the system's resilience. If such nodes are disturbed (e.g., through vegetation loss), it can lead to a significant increase in hydrological and sediment connectivity, making the system more vulnerable to further disturbances.

Betweenness Centrality (BC) represents a node's ability to act as a bridge (i.e. a connecting node along the pathways between nodes) during transportation processes. A node with high BC value has a high number of connected pathways passing through it and reaching other nodes in a network (Heckmann et al., 2015). The BC of node u is defined as:

$$BC_u = \sum_{i,j \neq u} n_{ij}(u) \tag{5}$$

where n_{ij} is the total number of shortest paths from node i to node j that pass through node u. Nodes with high BC act as critical conduits for resource flow, and their removal or disruption can fragment the network, reducing overall connectivity and resilience. Identifying these nodes allows for targeted management actions to enhance or protect key pathways that support the system's functioning.

Relative Node Efficiency (RNE) evaluates the impact of node removal on the overall connectivity of the system (Veremyev et al., 2015). This metric is potentially useful within the context of dryland geomorphology as it highlights locations within the landscape where we can most effectively manipulate the system to alter connectivity. Thus, the characteristics or attributes of nodes can be manipulated to either increase or decrease the connectivity of that node, and thus impact connectivity of the wider system.

$$RNE_u = \frac{GE_G - GE_H}{GE_G} \times 100 \tag{6}$$

where GE_G is the global efficiency of the network and GE_H is the network's global efficiency after node u is removed. Positive RNE values indicate that node removal reduces global efficiency, suggesting that the node is important for maintaining overall connectivity and resilience. Negative RNE values suggest that node removal increases GE, possibly by eliminating redundant or inefficient pathways. Understanding RNE is potentially useful in identifying nodes that are critical or detrimental to the system's resilience, guiding interventions to enhance network robustness.

To compare node-level network metrics between grassland and shrubland states, we apply a two-sample t-test, which allows us to determine if the mean values of a given metric differ significantly between ecosystems.

2.3.3. Connectivity relations: SC, FC_{hyd}, and FC_{sed}

We examine relations between SC, FC_{hyd}, and FC_{sed} in grassland and shrubland ecosystems using correlation analysis (Liégeois et al. 2020, Voutsa et al., 2021). We explore the correlations between nine node-level connectivity metrics: SC (WLOCOP, BC, RNE), FC_{hyd} (WLOCOP, BC, RNE), and FC_{sed} (WLOCOP, BC, RNE). This analysis provides insights into both intra-layer connectivity relations (i.e., SC-SC, FC_{hyd}-FC_{hyd}, and FC_{sed}-FC_{sed} for all combinations of WLOCOP, BC, RNE) and inter-layer connectivity relations (i.e., SC-FC_{hyd}, SC-FC_{sed}, and FC_{hyd}-FC_{sed} for all combinations of WLOCOP, BC, RNE).

For each pair of metrics, we calculate the Pearson correlation coefficient (r) to quantify the strength and direction of the relation. r values range from −1 to 1:

1. A value of 1 indicates a perfect positive correlation, meaning both variables increase together.
2. A value of −1 indicates a perfect negative correlation, meaning one variable increases while the other decreases.
3. A value near 0 indicates little to no linear relation between the variables.

High positive r values suggest a strong positive correlation between the metrics, indicating that the connectivity patterns captured by one metric are similar to those captured by the other. Conversely, low or negative r values suggest weak or inverse relationships between the metrics, indicating that the connectivity patterns differ.

High intra-layer correlations suggest that the different node-level metrics capture similar aspects of connectivity within a given layer, while low correlations indicate that the metrics capture different facets of connectivity. Inter-layer correlations offer insights into the relations between structural and functional connectivity, as well as the strength of coupling between water and sediment connectivity. High SC-FC correlations suggest that structural constraints strongly dictate functional connectivity, whereas lower correlations imply functional divergence from structure. Similarly, high FC_{hyd}-FC_{sed} correlations indicate a strong coupling between water and sediment connectivity, while low correlations suggest their decoupling.

By comparing the correlation coefficients between the different metrics and layers, we aim to gain a deeper understanding of how network structure relates to function under variable conditions and across alternate ecosystem regimes. This analysis will help quantify the complex interplay between structural and functional connectivity in grassland and shrubland ecosystems.

3. Results

3.1. Global scale characteristics over grassland and shrubland

The structural connectivity (SC) network for grassland has twice as many areas, compared with shrubland, where densely vegetated patches (cover >= 60 %) intersect with SC pathways causing them to become disconnected (Fig. 2a,b). This topological difference is reflected in the higher number of links for the shrubland SC network (954) compared to the grassland network (720) (Fig. 3). The spatial distribution of weighted links in the shrubland network is more uniform, with stronger links (weights close to 1) evenly distributed across the plot. In contrast, the grassland SC network exhibits high variation in link distribution (Fig. 3a,b). The SC-grassland network has a median link weight of ~ 0.8 with no outliers, whereas the SC-shrubland network has a median of 1 and numerous outlier weights from 0 to 0.9 (Fig. 3a,b).

Functional connectivity for both water (FC_{hyd}) and sediment (FC_{sed}) are highly sensitive to rainfall amount but less influenced by antecedent soil moisture (Fig. 3) across grassland and shrubland. Across both vegetation types, spatially, link weights intensify in downslope regions, achieving maximum values along the plots' lower boundaries under high rainfall (Fig. 2c-f). The FC_{sed} network is connected in upslope areas, unlike the FC_{hyd} network (Fig. 2e,f). While FC_{hyd} for grassland and shrubland have comparable link counts under heavy (45 mm) rainfall. Grassland FC_{hyd} and FC_{sed} drops sharply with decreasing rainfall, with the system being completely disconnected under moderate rainfall (15 mm). In contrast, the shrubland FC_{hyd} network retains connectivity at 10 mm rainfall (Fig. 3b). The grassland FC_{hyd} network also exhibits a narrower distribution and fewer high-weight outliers compared to the shrubland (Fig. 3a,b). For FC_{sed}, the different vegetation types show similar link counts but more extreme weight outliers in the shrubland, indicating stronger sediment connectivity (Fig. 3c,d).

3.2. Global-level connectivity metrics

The centralization degree (CD) of the structural connectivity (SC) network is 0.0011 in grassland and 0.0013 in shrubland (Fig. 4a,b). The SC networks have comparable CD values of 0.005 in upslope areas for both ecosystems. However, CD increases to 0.02 in the shrubland downslope region versus 0.16 in the grassland (Fig. 4a,b). In terms of functional connectivity, shrubland exhibits uniformly higher CD for FC_{hyd} and FC_{sed} (Fig. 4i,j,q,r). For all FC networks, CD increases with rainfall amount and antecedent soil moisture in both ecosystems (Fig. 4a,b,i,j,q,r). However, CD increases more gradually as rainfall increases for FC_{hyd} compared to the sharper increase observed for FC_{sed} (Fig. 4i,j,q,r). For example, in the shrubland downslope, FC_{hyd} CD increases from 0.008 to 0.016 when rainfall increases from 24 mm to 45 mm under high soil moisture (Fig. 4j). Under the same conditions, FC_{sed} CD increases markedly from 0.002 to 0.013 (Fig. 4r).

Examining the relation between CD and total discharge shows that CD for FC_{hyd} increases linearly with total discharge in both ecosystems (Fig. 5a). The slope of this relation is steeper for shrubland, indicating that for the same level of total discharge, CD is higher in shrubland than in grassland. For FC_{sed}, both total sediment output and CD values are extremely low for rainfall totals of 24 mm and lower (Fig. 5e). A significant relationship is observed only at a rainfall total of 45 mm. Under these conditions, the relation between total sediment transport and CD is steeper for shrubland, while grassland shows a more gradual increase (Fig. 5e).The global efficiency (GE) of the SC network is 2.88 x 10ˆ-6 in the shrubland versus 1.10 x 10ˆ-6 in the grassland, i.e. GE for SC shrubland is 2.6 times greater than the GE for SC grassland (Fig. 4c,d). For high rainfall and high soil moisture, the GE of FC_{hyd} is 1.51 x 10ˆ-6 in grassland versus nearly twice that in shrubland (Fig. 4k,l). Similarly, the GE of FC_{sed} is approximately 3 times higher in shrubland (4.41 x 10–6) compared to grassland under these wet conditions (Fig. 4s,t). Overall, GE of FC networks is highly sensitive to rainfall and soil moisture, increasing under wetter states.

The relation between GE and total discharge or total sediment output parallels that observed for CD (Fig. 5b,f). GE increases more sharply with total discharge or total sediment output in shrubland compared to grassland.

The SC networks show weak positive assortativity for vegetation cover (AC-veg), with coefficients of 0.0635 in grassland and 0.1937 in shrubland (Fig. 4e,f), suggesting nodes have moderately similar vegetation densities. SC networks exhibit stronger disassortativity around −0.4 for microtopography (AC-topo), indicating connections between

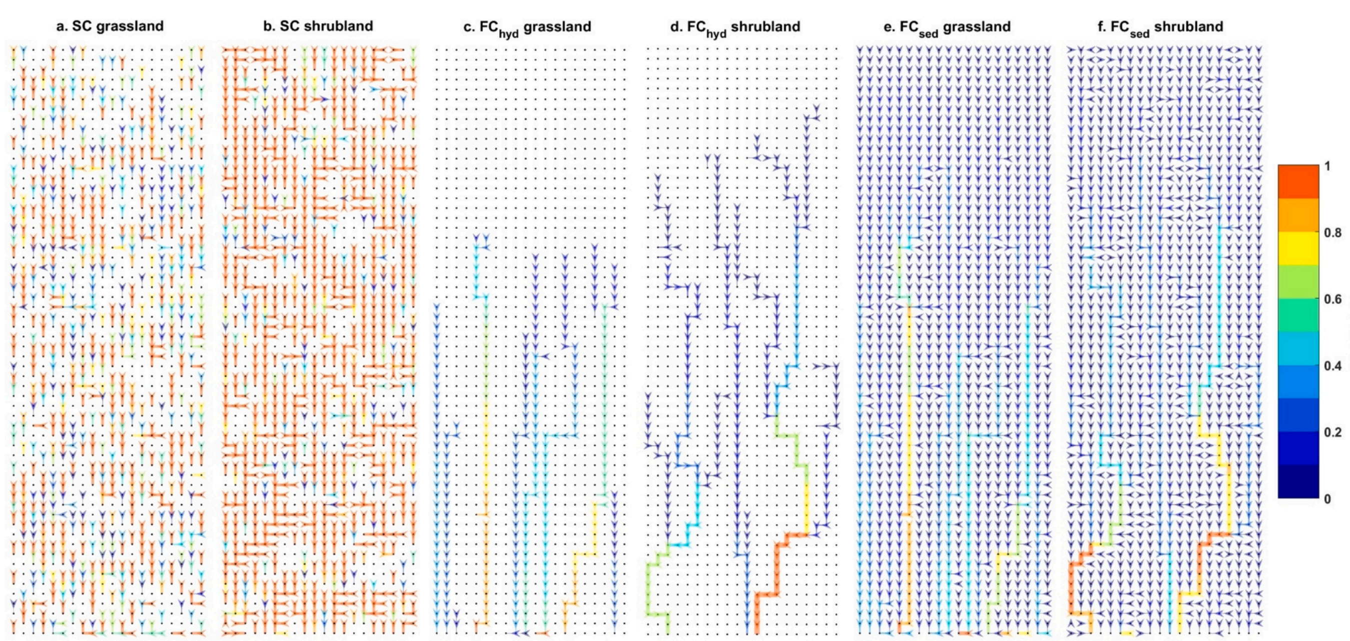

Fig. 2. Connectivity networks for grassland and shrubland plots. Structural connectivity networks for grassland (a) and shrubland (b). Functional connectivity networks for water (c and d) and sediment (e and f) under 45 mm rainfall total and high (21.1 %) soil moisture in grassland and shrubland plots, respectively (zoomed in high resolution plots are presented in the supplementary document).

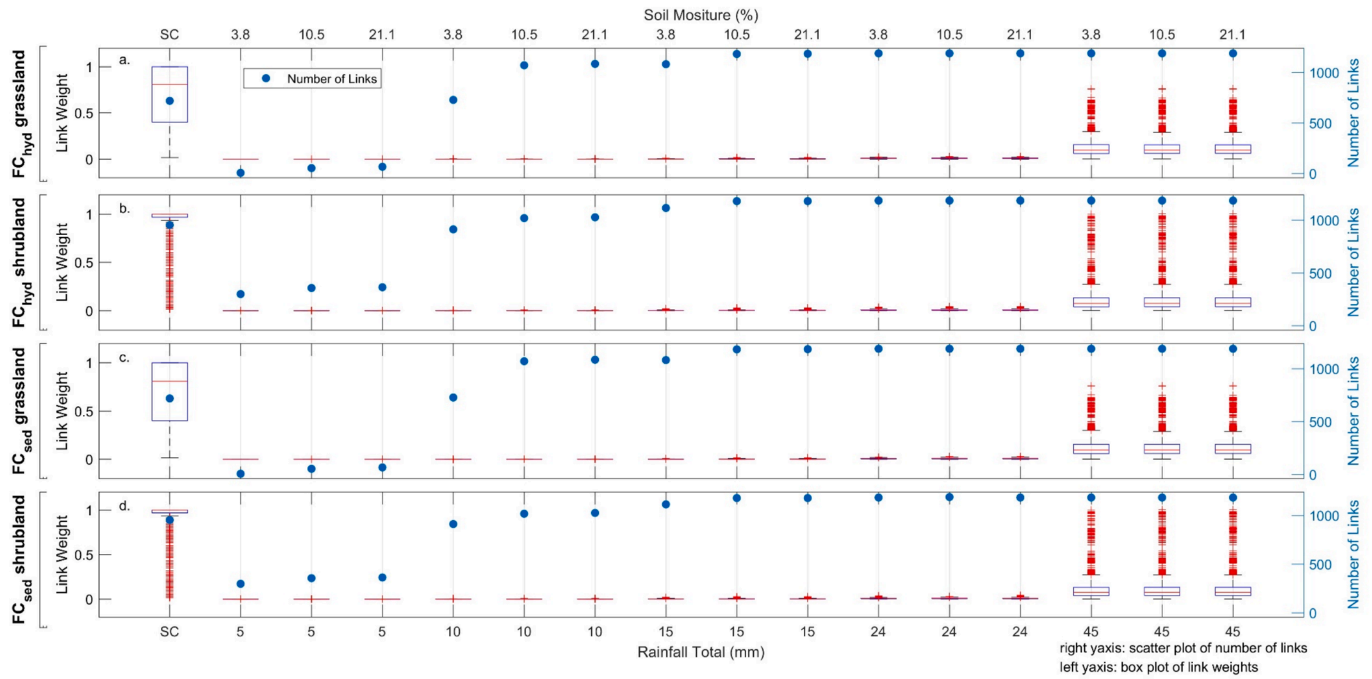

Fig. 3. Distributions and means of link weights across structural (SC) and functional connectivity (FC) networks. Boxplots on the left y-axis show the distribution of link weights for SC network (i.e. first boxplot in each four subplot a to d) and (a) FC_{hyd} networks in grassland, (b) FC_{hyd} networks in shrubland, (c) FC_{sed} networks in grassland, and (d) FC_{sed} networks in shrubland. Number of link weights are indicated by blue circular markers plotted on the right y-axis. FC networks were constructed under different rainfall conditions (lower x axis: 5 mm, 10 mm, 15 mm, 24 mm, 45 mm) and soil moisture levels (upper x-axis: 3.8 % low, 10.5 % medium, 21.1 % high). The boxplot whiskers indicate 1.5 times the interquartile range with outliers shown as red plus sign. Higher mean link weights arise under higher rainfall and soil moisture across all FC networks. (For interpretation of the references to colour in this figure legend, the reader is referred to the web version of this article.)

nodes of disparate relief (Fig. 4g,h). For FC networks, AC-veg remains near 0 in grassland but increases to ~ 0.2 for FC_{hyd} and ~ 0.4 for FC_{sed} in shrubland (Fig. 4m,n,u,v). Two exceptions are the highly negative AC-topo for FC_{hyd} in shrubland upslope (−0.7 in Fig. 4p) and positive values under low rainfall. Overall, AC-veg and AC-topo are independent of rainfall and soil moisture, instead depending on position in the directed network, with highest values in mid-slope areas that are more central within the network.

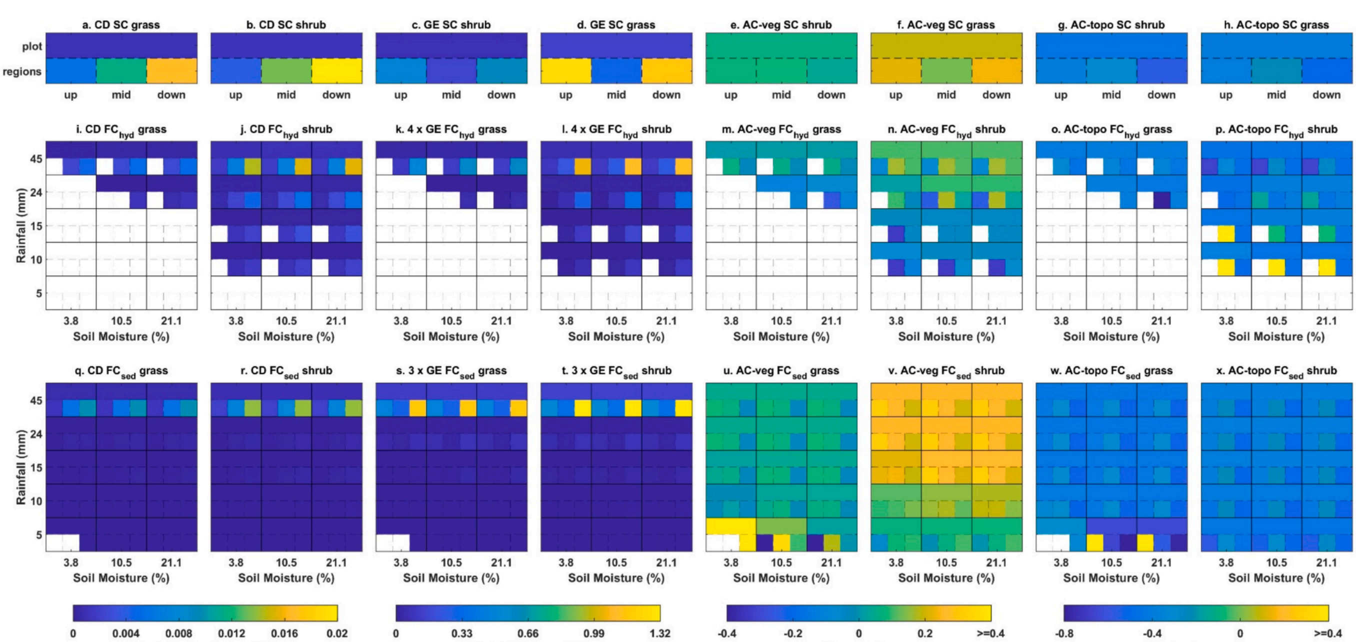

Fig. 4. Global-scale connectivity metrics for grassland and shrubland for SC and FC networks under different rainfall amounts and antecedent soil moisture. Four global-scale metrics i.e. Centralisation Degree, Global Efficiency, Assortativity Coefficient of percentage vegetation cover and Assortativity Coefficient of micro topography are presented for SC (a to h), FC_{hyd} (i to p) and FCsed network (q to x). The empty cell represents that network do not exist under the specified climate conditions.

The relation between AC-veg for FC_{hyd} and total discharge shows that AC-veg values increase and become positive as total discharge increases (Fig. 5c). This increase is steeper in shrubland, indicating that higher water flow is associated with stronger assortative mixing based on vegetation cover. In grassland, even under high total discharge, AC-veg remains close to zero, suggesting a lack of strong assortative mixing.

For FC_{sed}, the relation between AC-veg and total sediment output appears inconsistent, suggesting that AC-veg is relatively independent of total sediment transport (Fig. 5g). Regarding AC-topo, its relation with total discharge is inverse to that of AC-veg; AC-topo values become more negative as total discharge increases (Fig. 5d), indicating stronger disassortative mixing with higher water flow. For total sediment output, the relation of AC-topo mirrors that of AC-veg and is variable (Fig. 5h).

3.3. Node-level connectivity metrics

The mean Weighted Length of Connected Pathways (WLOCOP) is higher for the shrubland SC network at 4.98 m compared to 1.11 m in the grassland SC network (Fig. 6 d). The shrubland SC also shows greater variability in WLOCOP, with a standard deviation of 9.45 m versus 2.01 m for grassland SC. Visually, the shrubland SC exhibits a wider spread of WLOCOP values on the landscape (Fig. 6a-b). Similarly, the average Betweenness Centrality (BC) is over 10 times greater in the shrubland SC at 31.75 versus only 3.06 in the grassland SC (Fig. 6c-d). The shrubland SC has a much wider BC distribution as well, with a standard deviation of 76.66 versus just 9.44 in grassland SC. Higher BC suggests the shrubland SC contains more critical nodes acting as bridges for potential water transfers. However, the Relative Node Efficiency (RNE) is comparable between SC networks, with mean values close to zero in grassland SC (−0.080) and shrubland SC (−0.032). Both SC networks show an approximately normal RNE distribution centred on zero (Fig. 6e-f).

The mean WLOCOP is over four times higher in shrubland FC_{hyd}, (0.20 m) compared to grassland FC_{hyd} (0.05 m) under high rainfall conditions (Fig. 7a-b), which indicates that individual nodes are integrated into longer pathways, facilitating connected water transfer in shrublands. These values are much lower than the WLOCOP for the grassland and shrubland SC networks. The distribution of WLOCOP values is also wider in shrubland FC_{hyd} (std dev = 0.51 m) versus grassland FC_{hyd} (std dev = 0.15 m) (Fig. 7d). The average BC of nodes in the shrubland FC_{hyd} network (75.2) is an order of magnitude greater than the grassland FC_{hyd} network (7.4) (Fig. 7b-e). As with WLOCOP, the BC values in shrubland FC_{hyd} exhibit much greater variability (std dev = 157.7) than grassland FC_{hyd} (std dev = 20.2), indicating that nodes within the shrubland FC_{hyd} network act as critical bridges for water transfers across the landscape. In contrast, the Relative Node Efficiency (RNE) is comparable between grassland and shrubland FC_{hyd} networks, with both centered around zero (grassland mean = -0.13, shrubland mean = -0.11) (Fig. 7c,f). The RNE distributions are approximately normal for both vegetation states. The similar RNE indicates minimal differences in the closeness of node connections between grassland and shrubland FC_{hyd} networks.

The average WLOCOP is 3 times higher in shrubland FC_{sed} (0.38 m) versus grassland FC_{sed} (0.12 m) under high rainfall conditions (Figure a-b). The distribution of WLOCOP values is wider in shrubland FC_{sed} (std dev = 1.21 m) compared to grassland FC_{sed} (std dev = 0.33 m) (Fig. 8d). Similarly, the mean BC of nodes is nearly 10 times greater in shrubland FC_{sed} (47.2) relative to grassland FC_{sed} (4.8) (Fig. 8b-e). The BC distribution exhibits higher variability in shrubland FC_{sed} (std dev = 78.6) than grassland FC-sediment (std dev = 14.2), indicating that, as with the FC_{hyd} network, a higher number of nodes in the FC_{sed} network are key bridges for sediment transfers. The Relative Node Efficiency (RNE) distributions are comparable between grassland and shrubland FC_{sed} networks, centered close to zero for both grassland (mean = -0.08) and shrubland (mean = -0.07) (Fig. 8c,f), suggesting minimal differences in local connection density between the two vegetation states.

Comparisons of WLOCOP, BC, and RNE with spatial discharge and

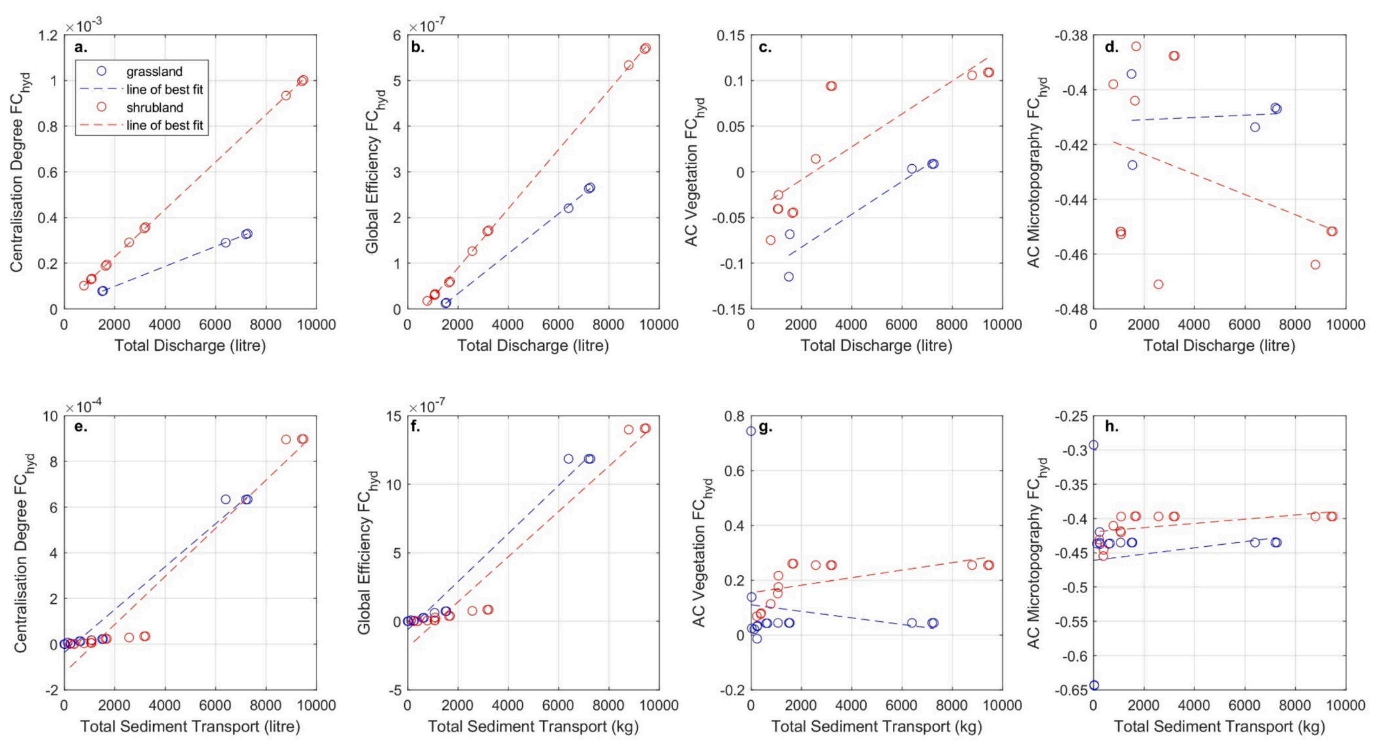

Fig. 5. Scatter plots showing the relations between global-scale metrics—(a, e) Centralization Degree (CD), (b, f) Global Efficiency (GE), (c, g) Vegetation Assortativity Coefficient (AC-veg), and (d, h) Microtopography Assortativity Coefficient (AC-topo)—and (a–d) total discharge and (e–h) total sediment transport at the hillslope outlet for functional connectivity networks of water (FChyd) and sediment (FCsed), respectively. Data points represent different rainfall events (5 mm, 10 mm, 15 mm, 24 mm, and 45 mm) and antecedent soil moisture conditions (low, medium, high) for grassland and shrubland ecosystems.

sediment transport at the node level show that shrubland tends to exhibit a wider range and higher maximum values for these metrics than grassland (Fig. 9). WLOCOP increases more rapidly with increasing discharge or sediment in shrubland compared to grassland (Fig. 9 a,d). While BC and RNE generally increase with higher discharge or sediment transport, nodes in high-flow or high-transport areas do not uniformly exhibit high BC or RNE, resulting in a broader and more variable.

distribution in shrubland (Fig. 9 a,b,e,f).

3.4. Structural and functional connectivity relations

Here, we analyse the relations between structural connectivity (SC) and functional connectivity of water (FC_{hyd}) and sediment (FC_{sed}) across grassland and shrubland for (1) intra-layer correlations (e.g., SC-SC, FC_{hyd}-FC_{hyd}, FC_{sed}-FC_{sed}) and (2) inter-layer correlations (e.g., SC-FC_{hyd}, SC-FC_{sed}, FC_{hyd}-FC_{sed}).

3.5. Intra-layer relations

In grassland with rainfall less than 45 mm rainfall, the intra-layer correlations within SC metrics (WLOCOP, BC, RNE) are mostly moderate, with some notable exceptions (Fig. 10). For instance, WLOCOP and BC exhibit a positive correlation of 0.42. However, negative correlations are also observed within SC metrics e.g., BC and RNE showing a negative correlation of −0.13. In shrubland ecosystems, under the same rainfall condition, strong intra-layer correlations are observed. SC metrics show strong positive correlations, with WLOCOP and BC having a correlation of 0.67.

FC_{hyd} metrics in grassland ecosystems demonstrate strong positive correlations under 45 mm rainfall, with BC and RNE showing a correlation of 0.61. Similarly, FC_{sed} metrics display strong intra-layer correlations, exemplified by a correlation of 0.86 between BC and RNE. For shrubland, FC_{hyd} metrics exhibit robust correlations, with BC and RNE showing a correlation of 0.88. FC_{sed} metrics maintain strong intra-layer correlations, with a correlation of 0.52 between WLOCOP and BC.

At 24 mm rainfall, the intra-layer correlations are strong for most metrics. As total event rainfall decreases, the general trend in both grassland and shrubland ecosystems is that intra-layer correlations within FC_{hyd} and FC_{sed} remain consistently strong. However, the presence of negative correlations within SC metrics indicates some complexity in how different metrics capture aspects of structural connectivity. Even at the lowest rainfall level of 5 mm, the strong intra-layer correlations persist within FC_{hyd} and FC_{sed} metrics in both ecosystems. Across the same rainfall amount, shrubland tends to demonstrate stronger intra-layer correlations than grassland (Fig. 10).

3.6. Inter-layer relations

In grasslands with rainfall less than 45 mm, the inter-layer correlations between SC and FC_{hyd} are moderate, with WLOCOP and BC showing a correlation of 0.42 (Fig. 10). The correlations between SC and FC_{sed} are weaker, with RNE and BC showing a correlation of 0.30, indicating some divergence between structural and sediment connectivity. Nonetheless, the correlations between FC_{hyd} and FC_{sed} remain strong, with a correlation of 0.67 between BC and BC, indicating a strong coupling between water and sediment connectivity.

When rainfall decreases to 24 mm, the pattern in inter-layer correlations in grassland ecosystems remains similar to 45 mm. SC-FC_{hyd}

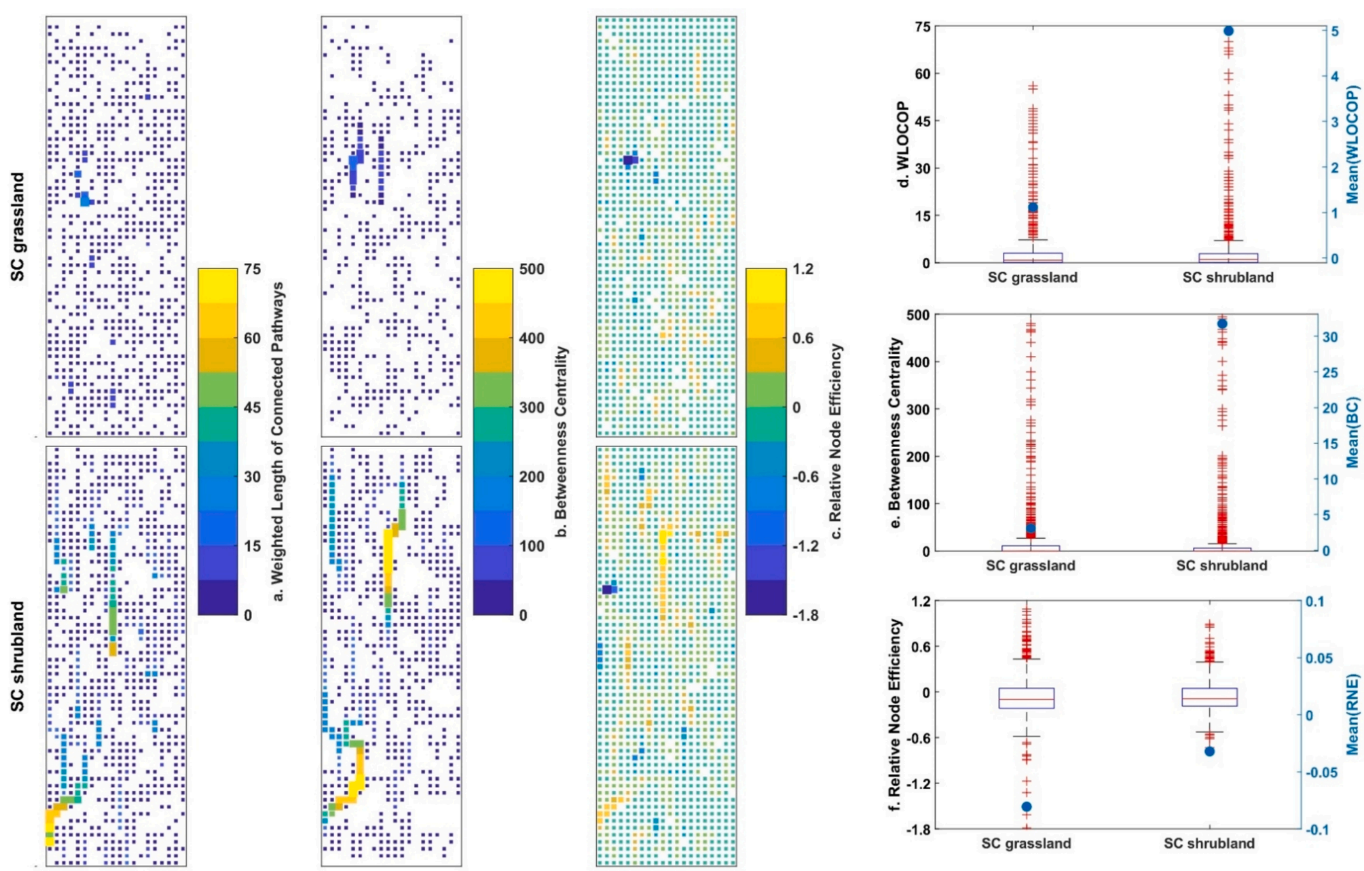

Fig. 6. Local-scale connectivity metrics for structural connectivity network. Three local-scale metrics i.e. Weighted Length of Connected Pathways, Betweenness Centrality and Relative Node Efficiency are presented for grassland and shrubland plots. The spatial plots (a to c) visualize the metric value of each node on the landscape, with size of the nodes weighted based on the associated metric value. The boxplots (d to f) show the distribution of values across all nodes for grassland and shrubland.

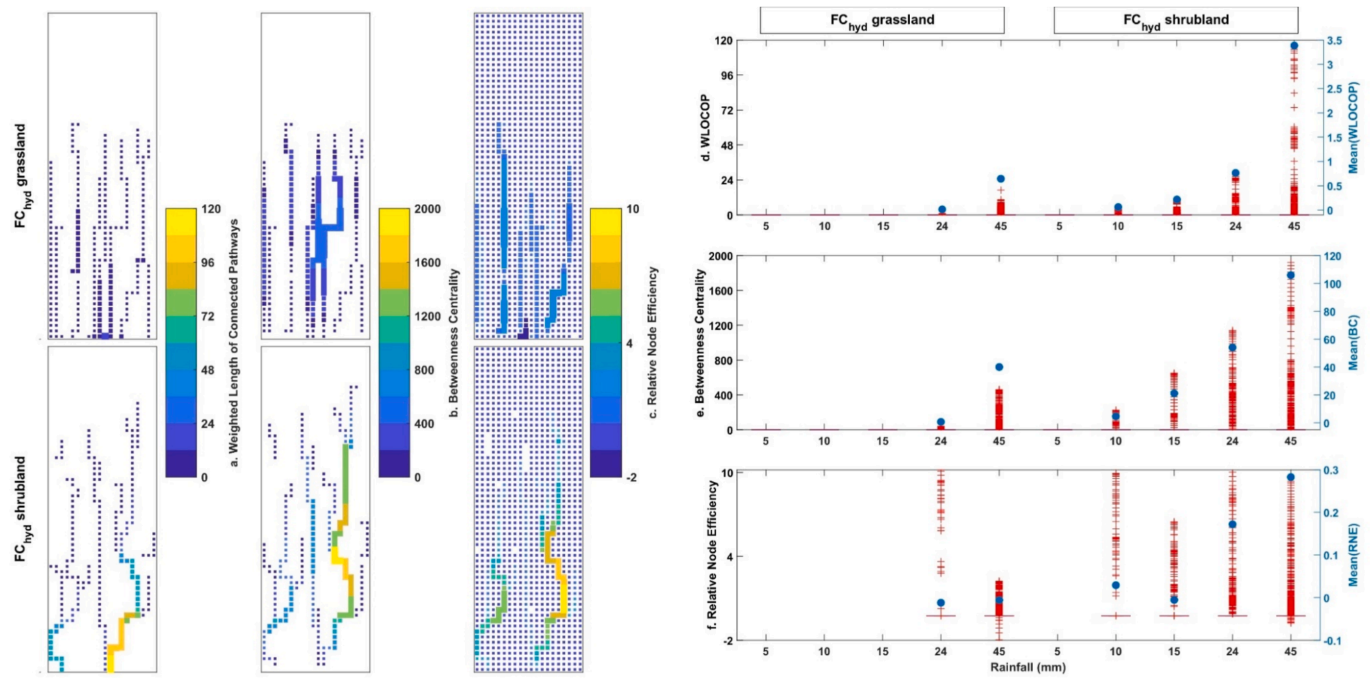

Fig. 7. Local-scale connectivity metrics for functional connectivity of water (FC$_{hyd}$) network. Three local-scale metrics i.e. Length of Connected Pathways Weighted, Betweenness Centrality and Relative Node Efficiency are presented for grassland and shrubland plots. The spatial plots (a to c) visualize the metric value of each node on the landscape under high rainfall total (45 mm) and high antecedent soil moisture condition (21.1 %), with size of the nodes weighted based on the associated metric value. The boxplots (d to f) show the distribution of values across all nodes for different amount of rainfall totals (5 mm, 10 mm, 15 mm, 24 mm and 45 mm).

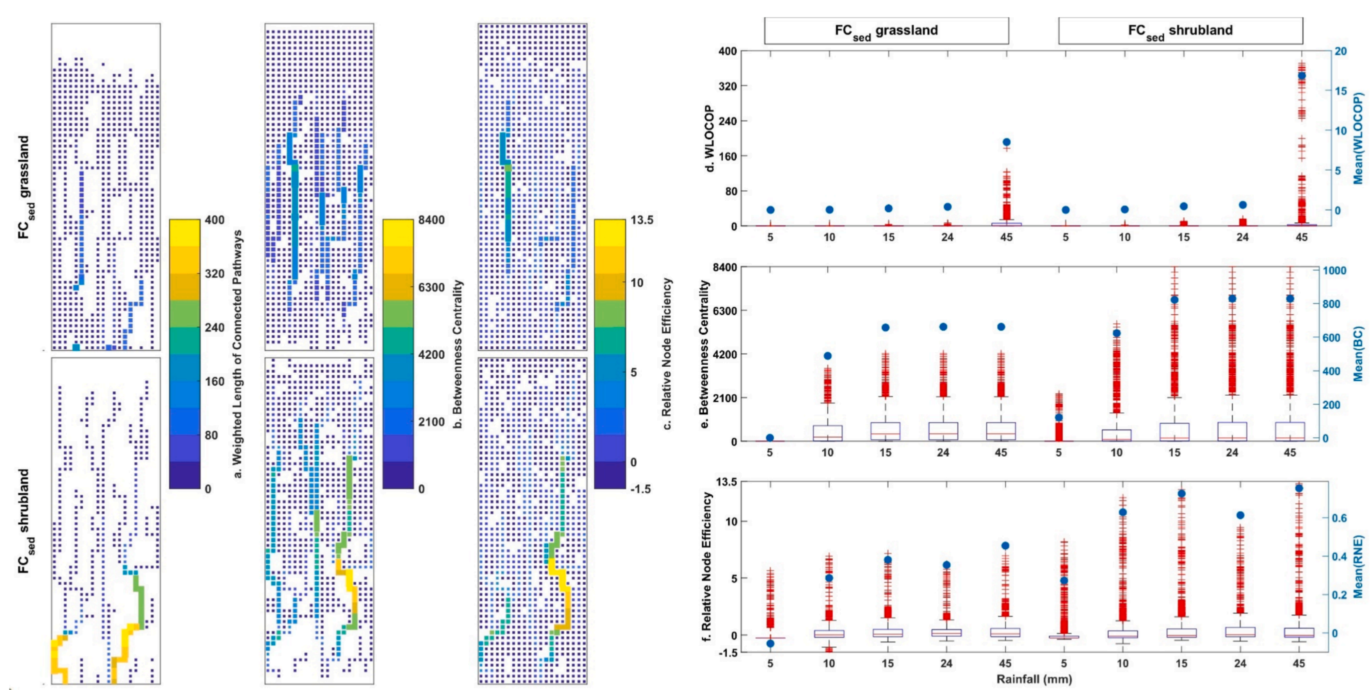

Fig. 8. Local-scale connectivity metrics for functional connectivity of sediment (FC$_{sed}$) network. Three local-scale metrics i.e. Length of Connected Pathways Weighted, Betweenness Centrality and Relative Node Efficiency are presented for grassland and shrubland plots. The spatial plots (a to c) visualize the metric value of each node on the landscape under high rainfall total (45 mm) and high antecedent soil moisture condition (21.1 %), with the size of the nodes weighted based on the associated metric value. The boxplots (d to f) show the distribution of values across all nodes for different amounts of rainfall totals (5 mm, 10 mm, 15 mm, 24 mm and 45 mm).

correlations continue to be moderate, SC-FC$_{sed}$ correlations remain weaker, and FC$_{hyd}$-FC$_{sed}$ correlations persist as strong. In both vegetation types, a lower rainfall tends to reduce the strength of SC to FC$_{hyd}$ correlations, particularly noticeable at the lowest rainfall level of 5 mm, where SC appears least influential on FC$_{hyd}$. Even with variations in total event rainfall, the correlation between FC$_{hyd}$ and FC$_{sed}$ remains consistently strong across all rainfall and soil moisture conditions in both ecosystems, underscoring the tight coupling between hydrological

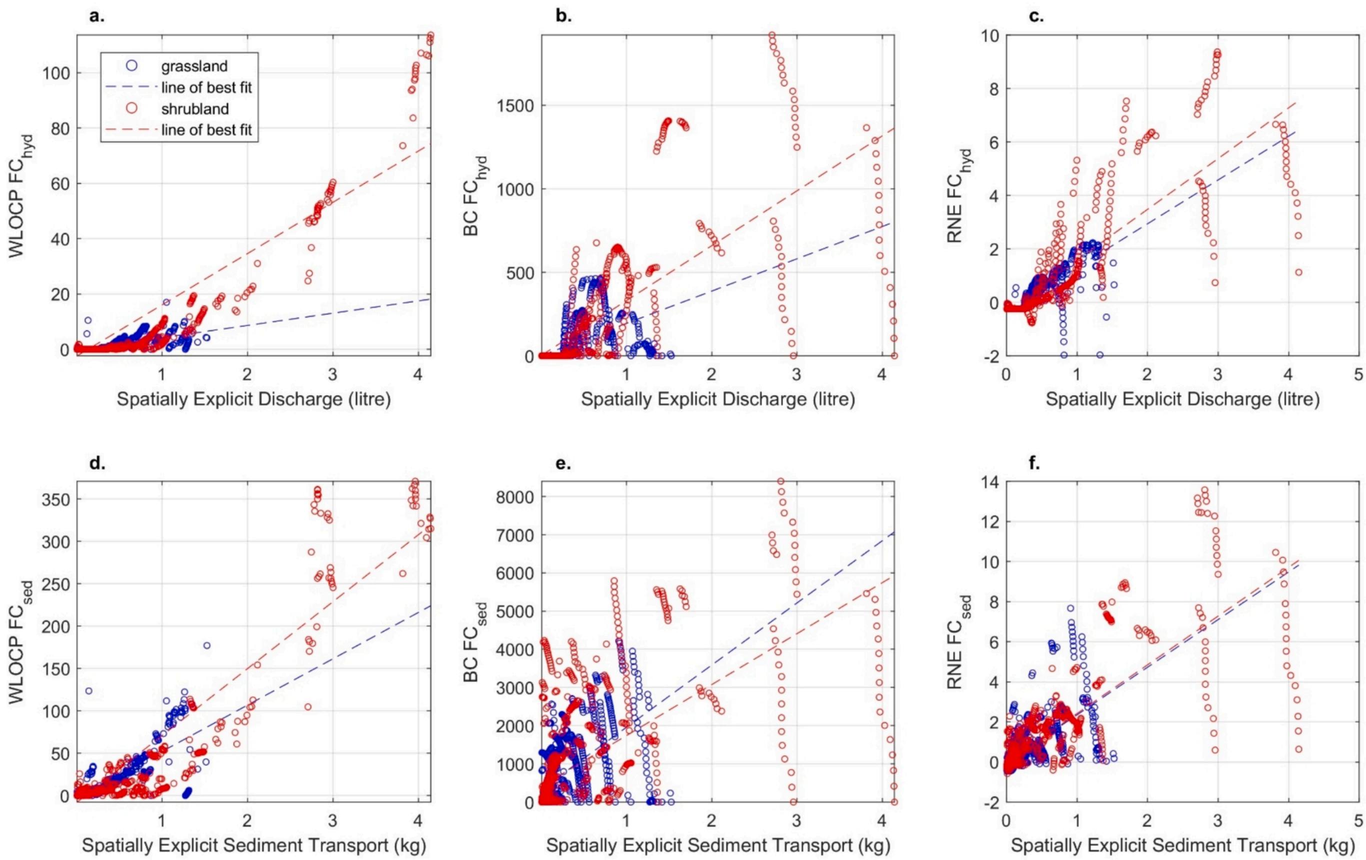

Fig. 9. Scatter plots showing relations between local-scale metrics under high rainfall total (45 mm) and high antecedent soil moisture condition (21.1 %)—Weighted Length of Connected Pathways (WLOCP), Betweenness Centrality (BC) and Relative Node Efficiency (RNE)—with spatially explicit output of discharge (a–c) and sediment transport (d–f) for the functional connectivity networks of water (FC_{hyd}) and sediment (FC_{sed}), respectively.

connectivity and sediment connectivity.

4. Discussion

In this study, we utilized network metrics to examine differences in connectivity across grassland and shrubland hillslopes. We quantified the structural connectivity (SC) of these landscapes to investigate how it influences functional connectivity (FC). Our analysis distinguished between hydrological functional connectivity (FC_{hyd}) and sediment functional connectivity (FC_{sed}), focusing on their responses to variations in vegetation type and environmental conditions, such as event rainfall and antecedent soil moisture. Initially, we analyzed the global and local-scale characteristics of SC and FC. We then explored the types and strengths of SC-FC relations within grassland and shrubland hillslopes.

4.1. Local connectivity patterns

The network analysis presented in this study provides a comprehensive quantification of the extensive reworking of localized connectivity patterns associated with the transition from grassland to shrubland ecosystems (Figs. 6-8).

Node-level metrics, particularly WLOCOP, provide quantitative evidence about where (i.e. spatial locations) and when (i.e. under which environmental conditions) shrub encroachment fundamentally alters local connectivity, echoing previous observations (Wainwright et al. 2002a, Turnbull et al. 2008, and Okin et al. 2009). These changes concentrate flow and modify resource distribution, fundamentally altering the landscape's ecological dynamics (Bestelmeyer et al., 2011). The quadrupled increase in SC, characterised by the WLOCOP (Fig. 6), demonstrates a clear shift in network topology between grassland and shrubland hillslopes, likely shaped by long-term structural–functional feedbacks (Crompton et al., 2023; Maestre et al., 2016; Turnbull & Wainwright, 2019; Voutsa et al., 2021).

Furthermore, our analysis of FC_{hyd} and FC_{sed} also shows a distinct difference in WLOCP between the grassland and shrubland hillslopes, but only for the larger rainfall events and wetter antecedent soil moisture conditions that amplify the runoff and erosion response of the system (Turnbull et al., 2010b). Notably, WLOCP is higher over shrubland for moderate events (e.g. total event rainfall 10 mm), indicating the connectivity of water and sediment over greater distances in comparison with the same rainfall event over grassland where a mean WLOCOP close to 0 indicates virtually no redistribution of resources along connected edges between nodes.

Betweenness Centrality (BC) further identifies nodes within the network where numerous flow pathways both converge and diverge, highlighting their strategic importance in the control and distribution of flows throughout the system. Higher BC values in shrublands for SC and FC (Figs. 6-8) highlight the emergence of critical flow pathways in the intershrub areas via SC-FC feedbacks, that become persistent and resilient features within the system (Turnbull et al., 2008). In essence, SC-FC feedbacks – induced by a change in vegetation and concurrent changes in microtopography and soil properties – causes a change in the network structure, essentially rewiring the system by favouring well-developed pathways in intershrub areas (Wainwright et al., 2002). Enhanced runoff-runon dynamics underpin the increased node-level connectivity metrics (WLOCP, BC), reflecting the capture or channelization of resources by vegetated patches, depending on the microtopography of the vegetated patches. This phenomenon generates substantial heterogeneity in partitioning and timing of resource transfer (Mayor et al., 2013), with scattered zones of concentrated and well-connected flows (Figs. 7-

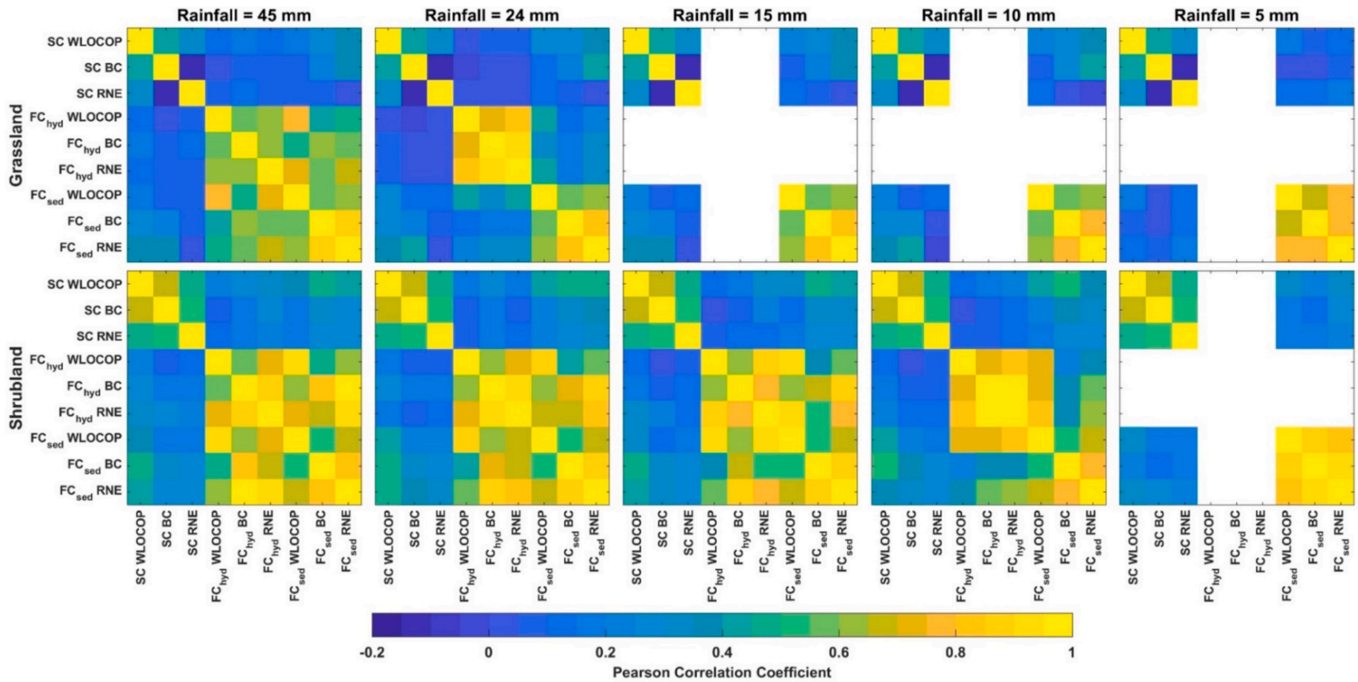

Fig. 10. Correlation matrices showing the relations between nine node-level connectivity metrics for grassland (top row) and shrubland (bottom row) ecosystems under five rainfall events: 45 mm, 24 mm, 15 mm, 10 mm, and 5 mm (columns). The nine metrics include: Weighted Length of Connected Pathways (WLOCOP), Betweenness Centrality (BC), and Relative Node Efficiency (RNE) for structural connectivity (SC); and similar metrics for functional connectivity of water (FC_{hyd}), and functional connectivity of sediment (FC_{sed}). Each subplot displays the Pearson correlation coefficients (r) between all pairs of metrics, with colour intensity indicating the strength and direction of the correlation. Intra-layer correlations (SC-SC, FC_{hyd}-FC_{hyd}, and FC_{sed}-FC_{sed}) and inter-layer correlations (SC-FC_{hyd}, SC-F_{sed}, and FC_{hyd}-FC_{sed}) are represented within each subplot. Empty cells denote conditions where no network exists under the specified climate conditions. The main diagonal values in each subplot are always 1, as they represent the correlation of a metric with itself. All correlations are presented for high soil moisture conditions and are statistically significant (where p-value < 0.05). The intra-layer SC relations do not depend on rainfall amount.

8). Importantly, our results reveal that the extremely high WLOCOP and BC values remain localized along long connected pathways (Figs. 6-8), failing to propagate broader connectivity collapse over the entire hillslope i.e. majority of nodes have a high value of WLOCP and BC. This finding of localised connectivity patterns contrasts with the notion of widespread connectivity breakdown in shrublands and instead highlights the presence of critical nodes where localized modifications could drive broader connectivity shifts to support restoration or resilience (Maestre et al., 2016a; Scheffer and Carpenter, 2003; Turnbull et al., 2012).

Additional insights into local connectivity patterns emerge from examining how node-level metrics vary with local discharge and sediment transport at the scale of individual nodes (Fig. 9). WLOCOP increases exponentially with spatial discharge in shrubland, whereas in grassland the relation is more moderate, suggesting that shrub-dominated areas develop stronger localized connectivity under similar forcing conditions. A similar pattern is observed for sediment transport, where shrubland nodes display steeper increases in WLOCOP, indicating that these nodes can rapidly become key conduits for resource flow as sediment fluxes rise (Mayor et al., 2013; Okin et al., 2009).

In contrast, BC and RNE exhibit more variable and irregular relations with spatial discharge and sediment transport. Although higher discharge or sediment flux often corresponds to higher BC and RNE values, nodes with low BC and RNE persist even within high-flux areas. This scattered distribution implies that local-scale connectivity in shrublands remains heterogeneous, with certain nodes attaining disproportionately high importance only under specific conditions. The broader variability and extreme values observed in shrubland FC networks highlight their enhanced sensitivity to changes in local resource inputs. Such patterns could inform targeted management interventions, for instance, stabilizing key nodes in shrubland areas to reduce vulnerability to localized erosion or to improve resource retention and distribution (Turnbull and Wainwright, 2019).

4.2. Global connectivity patterns

Despite the extensive reorganization of local connectivity patterns, our analysis reveals distinct but less drastic differences in the global network properties of both grassland and shrubland ecosystems for all connectivity types: SC, FC_{hyd}, and FC_{sed}. The SC networks for grassland and shrubland exhibit differences in link densities and global efficiencies (Fig. 4), indicating that the overall network topology, at larger spatial scales, is influenced by vegetation structure (Crucitti et al., 2003). Specifically, the GE of the SC network in shrubland (2.88 x 10^{-6}) is higher than in grassland (1.10 x 10^{-6}), suggesting a more efficient resource distribution system in shrubland under the assessed conditions. Furthermore, the GE for FC_{hyd} is approximately three times higher in shrubland compared to grassland under high rainfall and soil moisture conditions. This pattern reflects a greater efficiency in hydrological connectivity in shrubland. Similarly, for FC_{sed}, the GE significantly increases with rainfall, indicating that sediment connectivity is highly sensitive to precipitation variations. This finding aligns with empirical observations of long-term stability in grass-to-shrub boundary dynamics (Peters et al., 2020), indicating that the network's inherent properties allow for the redirection of resource flows around localized disturbances.

The Centralization Degree (CD) within the SC network remains low in both grassland (0.0011) and shrubland (0.0013), reinforcing the decentralized nature of these networks, which enhances their resilience by facilitating the rerouting of resources in response to disturbances (Fig. 4). This low degree of centralization supports ecological stability on dryland hillslopes by distributing connectivity and reducing vulnerability to localized disruptions (Newman, 2006; Turnbull et al., 2008; Wainwright et al., 2002). However, CD in FC_{hyd} and FC_{sed} networks, while generally low, shows a slight increase with rainfall. This variation indicates a dependency on hydrological and sedimentary dynamics for connectivity centralization, particularly noted in shrubland where CD values rise more distinctly with increased precipitation.

A notable trend is the increase in CD from the upslope to the downslope regions across all three network types (SC, FC_{hyd}, and FC_{sed}). In both ecosystems, this upslope-to-downslope increase suggests that lower areas tend to assume more central roles, likely due to gravity-driven processes that enhance both water and sediment flow downward (Bracken and Croke, 2007). However, the increase in CD is significantly more pronounced in shrubland than in grassland. This pronounced effect highlights the influence of vegetation structure on connectivity dynamics, where shrubs potentially act as focal points for resource accumulation, intensifying the flow convergence and connectivity in downslope regions (Abrahams et al., 1995; Dickie and Parsons, 2012; Turnbull and Wainwright, 2019; Wilcox et al., 2022).

Despite these variations, the resilience of the global network topology − referring to the overall interconnectivity and efficiency of the networks − can be attributed to the presence of path redundancy. In the context of this system, path redundancy means that multiple pathways exist for resource flow, so if one pathway is blocked or disrupted, others can take over the function, ensuring continuous connectivity. This redundancy enables the networks to reroute resource flows when critical nodes are disrupted (Eichel et al., 2023, 2016; Ventresca and Aleman, 2015), a key mechanism that maintains functionality despite significant changes in local connectivity patterns (Figs. 6-8)). For instance, during heavy rainfall, shrub encroachment might block certain flow paths, but the presence of multiple pathways ensures that water and sediment can still reach downslope areas, albeit through different routes. This adaptability is particularly crucial in dryland landscapes, known for their pulsed resource inputs, where path redundancy ensures stability amid environmental fluctuations (Bestelmeyer et al., 2013). The marked resilience is evident not only in maintaining the global network structure but also in the networks' ability to adapt locally. As individual patches within shrublands undergo reconfiguration, alternative pathways are created, preserving essential network capacities and underscoring the networks' capacity to withstand vegetation shifts and associated redistributions of resources (Okin et al., 2009; Turnbull and Wainwright, 2019). This dynamic interplay between local adjustments and global stability highlights the critical role of path redundancy in sustaining ecological functions across arid landscape conditions.

Furthermore, the modular structure of the networks over grassland and shrubland, characterized by the presence of disconnected subnetworks (low CD and GE values), enhances the overall resilience of the system by limiting the propagation of disturbances such as concentrated erosion events across the entire network (Bodin and Norberg, 2007; Krause et al., 2003; Newman, 2006). This compartmentalization is particularly important in dryland ecosystems, where the spatial heterogeneity of vegetation and soil properties can create natural barriers to connectivity (Okin et al., 2009).

The observation that local differences in connectivity do not significantly affect the global network properties suggests that the system has a high degree of modularity or compartmentalization (Newman, 2006). This network structure is defined by semi-autonomous subnetworks capable of independently adjusting to local environmental changes, thereby safeguarding the broader network functionality (Bodin and Norberg, 2007; Krause et al., 2003). This aspect of compartmentalization is crucial, particularly in dryland ecosystems where the spatial heterogeneity of vegetation and soil properties can act as natural barriers that control connectivity (Okin et al., 2009). This modular design not only aids in resilience to environmental variability but also effectively limits the propagation of disturbances, such as concentrated erosion events and invasive species spread, across the entire network. By isolating these disturbances, the network prevents widespread ecological impacts, ensuring that localized disruptions do not escalate into systemic failures. This capacity to contain disturbances enhances the system's overall resilience, maintaining ecological function and stability even under conditions of environmental stress.

The uniform near-zero assortativity coefficient points to factors beyond the studied traits such as high vegetation densities or microtopographic relief primarily govern network positioning. While the assortativity for vegetation cover is weakly positive in SC networks of both grassland (AC-veg = 0.0635) and shrubland (AC-veg = 0.1937), suggesting a subtle preference for structural connectivity between nodes with similar vegetation densities, the effect is not pronounced. This variation underscores the impact of specific environmental conditions, such as sediment transport dynamics and hydrological connectivity, on vegetation-driven network formation. Conversely, the assortativity for microtopography in the SC network is strongly disassortative (AC-topo around −0.4), highlighting that structural connections frequently occur between nodes with significantly different relief. This pattern is especially pronounced in the FC_{hyd} networks of shrubland, where the AC-topo reaches −0.7 in upslope areas, indicating a dominant influence of topographic relief over vegetative similarity in determining connectivity. In FC networks within grasslands, the vegetation assortativity coefficient is close to zero, indicating a lack of correlation between connectivity and vegetation density. This suggests that areas of differing vegetation densities are just as likely to be connected as areas with similar densities. However, in shrubland, the coefficients for FC_{hyd} and FC_{sed} increase to approximately 0.2 and 0.4, respectively, indicating a stronger tendency for connectivity among nodes with similar vegetation under these conditions. This variation underscores the impact of specific FC type, such as FC_{hyd} and FC_{sed}, on vegetation-influenced connectivity network formation.

These results collectively suggest that geographic proximity, driven by topography, primarily dictates connections within these networks, overriding localized vegetative patterns. However, the central position within the directed network, particularly in mid-slope areas, exerts a significant influence, with assortativity varying independently of external factors like rainfall and soil moisture.

Further insights into global connectivity patterns emerge when considering the relations between global metrics and total resource outputs (Fig. 5). As total discharge increases, both CD and GE rise more steeply in shrubland than in grassland, indicating that shrub-dominated hillslopes translate higher runoff volumes into more centralized and efficient connectivity configurations. Similar trends are observed for total sediment export, where significant increases in CD and GE in shrubland occur primarily under the highest rainfall scenarios. These findings suggest that vegetation structure strongly modulates the response of network-level connectivity to hydrological forcing, echoing previous studies that link vegetation transitions to altered erosion and runoff regimes (Bestelmeyer et al., 2018; Bracken et al., 2015; Turnbull et al., 2008). Moreover, the contrasting responses of AC-veg and AC-topo to increasing discharge underscore that different structural attributes influence connectivity dynamics in distinct ways. While AC-veg tends to shift from neutral to more positive values in shrubland as discharge intensifies, AC-topo becomes increasingly negative, reinforcing the key role of topographic variation in shaping network organization (Caylor et al., 2009; Okin et al., 2009).

4.3. *Structure-Function relations*

A unique insight afforded by the network-based connectivity analysis is illuminating when and how landscape structure governs ecosystem functioning. By quantifying the relations between the structural connectivity (SC) and functional connectivity (FC) of water and sediment, we can better understand the complex connectivity dynamics across scales and process domains.

Our results show that sediment connectivity (FC_{sed}) exhibits a much tighter coupling to system structure (SC) than hydrologic connectivity (FC_{hyd}) (Fig. 8). This difference can be attributed to the distinct governing processes of sediment and water transport (Parsons et al., 1994;

Turnbull et al., 2010a). Sediment transport is primarily linked to topography and has low mobilization thresholds due to processes of raindrop erosion, which includes both raindrop detachment and splash (Wainwright et al., 2002). As a result, sediment flows are more readily trapped and channelled by structural landscape factors, and these structural legacies can persist for years, shaping observed sediment transfers even following major storm events (Nichols et al., 2018).

In contrast, hydrological connectivity shows a more dynamic response to variable rainfall, indicating a degree of independence from static landscape structures during active rainfall period (Wainwright et al., 2002). This finding challenges the common conceptual model that identifies topography and surface cover mosaics as the principal factors governing water redistribution (Thompson et al., 2014). However, it is important to clarify that this relative independence of FC_{hyd} from landscape structure is specifically noted during active rainfall. In the absence of precipitation, landscape structure predominates, influencing water movement significantly. Thus, the activation of FC_{hyd} is highly conditional, depending on rainfall presence and intensity.

Our results suggest that infiltration excess and saturation excess runoff processes respond more directly to variable precipitation characteristics than to static landscape boundaries. It is important to note that the flow routing in the model used in this study is based on steepest descent, which means that hydrologic connectivity is not entirely decoupled from the landscape structure. However, our analysis of the relation between structural and functional connectivity for different rainfall events (Fig. 10) reveals that the strength of the coupling between structure and function can vary depending on the magnitude of the rainfall event. This finding highlights the importance of considering the temporal dynamics of connectivity in dryland ecosystems, where the frequency and intensity of rainfall events can have a significant impact on resource redistribution (Turnbull et al., 2012). For example, under sufficiently large flows, "structurally disconnected areas" due to vegetation sinks can become hydrologically connected, demonstrating how extreme events can temporarily override structural constraints (Turnbull and Wainwright, 2019). These findings that larger, more intense rainfall events can temporarily override structural constraints and enhance SC-FC feedbacks (Fig. 10) have important future implications. As climate projections suggest an increase in the frequency and intensity of extreme rainfall events in many dryland regions (IPCC, 2021), the role of rainfall-driven processes in shaping connectivity may become even more pronounced. Under more frequent large flows, the coupling between structure and function could strengthen, leading to greater resource redistribution, enhanced erosion potential, and more dynamic connectivity regimes. This shifting baseline of connectivity in response to climate change highlights the need for adaptive management strategies—those that anticipate increases in event magnitude and target key structural elements to mitigate erosion risk, maintain resource retention, and preserve ecosystem resilience (Turnbull and Wainwright, 2019; Turnbull et al., 2012).

This nuanced understanding of SC-FC interactions is further refined by integrating metrics such as betweenness centrality (BC) and relative node efficiency (RNE), advancing previous methodologies that compared SC and FC using indices like the Relative Connectivity Index (Turnbull and Wainwright, 2019).

Our analysis indicates that both intra-layer and inter-layer correlations vary with rainfall intensity. In grassland and shrubland ecosystems, strong intra-layer correlations persist within FC_{hyd} and FC_{sed} across different rainfall conditions, suggesting a robust internal coherence in how water and sediment are processed within each connectivity domain. Inter-layer correlations, however, illustrate that while structural connectivity moderately influences hydrological processes, its impact on sediment connectivity is more pronounced.

These insights confirm that the structure–function relations in dryland ecosystems are not only complex but also highly dependent on specific resource dynamics. For sediment, structural constraints significantly govern redistribution; however, water flows demonstrate greater adaptability, capable of rerouting to maintain functionality despite disruptions. This differential responsiveness underscores the importance of targeted management strategies that can selectively address sediment and water connectivity to mitigate soil erosion while ensuring essential resource distribution within these fragile ecosystems.

4.4. From understanding to Action

Our improved understanding of connectivity dynamics in these systems using network-based metrics has great potential to inform targeted management actions. The insights gained from this study can guide specific interventions tailored to the distinct connectivity patterns of grassland and shrubland ecosystems. Turnbull et al. (2012) proposed enhancing resource retention in grasslands and manipulating flow paths in shrublands, and our network-based approach provides a quantitative framework for optimizing their implementation and evaluating the effectiveness of such interventions.

Our findings underscore the utility of local-scale connectivity metrics, such as WLOCOP and betweenness centrality (BC), which have demonstrated clear differences between grassland and shrubland ecosystems. These local metrics are highly responsive to vegetation transitions, making them valuable for detecting early warning signals of ecological regime shifts (Kéfi and Couteron, 2018). For example, a systematic increase in BC might indicate an emerging connectivity pattern that could precede significant ecosystem changes, offering managers a crucial window for intervention to prevent or mitigate potential declines in ecosystem health.

While global network metrics like global efficiency did not exhibit drastic differences between the two states, they provide a broad view of system stability. However, the more pronounced local connectivity changes observed in shrublands suggest that interventions at this scale might be more impactful (Peters et al., 2020; Turnbull and Wainwright, 2019). It is critical, however, to consider that altering connected flow paths in shrublands could paradoxically enhance the connectivity of degraded states, potentially stabilizing undesirable conditions.

More broadly, the network-based framework presented here serves as a blueprint for exploring connectivity dynamics across diverse spatiotemporal contexts (Tiwari et al., 2024). The approach demonstrated here for end-member vegetation states points to the potential of local-scale connectivity metrics characterize patterns and reorganization rates in systems undergoing changes in vegetation state, potentially providing new insights into the role of connectivity in driving regime shifts (Turnbull et al., 2008) and the early warning signals that may precede them (Peters et al., 2006). Our multi-scale approach, which quantifies connectivity at both local and global scales (Figs. 3–7), is particularly well-suited for this type of comparative analysis, as it captures the complex interactions between fine-scale processes and landscape-level patterns. While global metrics provide a snapshot of overall system stability, local metrics offer actionable insights that can guide more precise and effective management interventions.

The network-based framework developed in this study provides a robust approach for exploring the multi-scale connectivity dynamics in dryland ecosystems (Bestelmeyer et al., 2011; Hervías-Parejo et al., 2020; Jacquet et al., 2022; Kleineberg et al., 2016; Maestre et al., 2022; Pilosof et al., 2017). Future research could extend this approach to investigate the impacts of different types of disturbances, such as fire or grazing, on connectivity patterns and resilience (Okin et al., 2009; Saco et al., 2020). The integration of additional data sources, such as remote sensing imagery could help us to validate the observed structural connectivity patterns at larger spatial scales (Mueller, 2014).

Moreover, the application of the network-based framework to other dryland ecosystems, such as savannas or steppes, could provide valuable insights into the generality of the patterns and processes identified in this study (Caylor et al., 2009; King et al., 2012). Comparative analyses across different ecosystems could help to identify common principles and mechanisms that govern connectivity and resilience in drylands, as well as to highlight the unique features and challenges of each system (Maestre et al., 2022).

Finally, the integration of the network-based approach with other modelling frameworks, such as agent-based models or ecosystem service models, could provide a more comprehensive understanding of the complex interactions between connectivity, ecosystem function, and human well-being in dryland landscapes (Bodin and Saura, 2010; James et al., 2013). Such integrated models could inform the development of more sustainable and resilient land management strategies that balance the needs of both people and nature in these fragile and dynamic ecosystems.

5. Conclusion

This research highlights the effectiveness of network-based approaches in unraveling the complex connectivity dynamics that underpin dryland resilience. Employing a weighted, directed network methodology has allowed us to quantify changes in system connectivity across multiple scales comprehensively. This network-based approach goes beyond simplistic binary metrics to capture the dynamics in connectivity pathways and reveals significant changes in local connectivity patterns during the transition from grassland to shrubland ecosystems.

Our analysis has allowed a comprehensive, quantitative assessment of variations in structural and functional connectivity across grassland and shrubland, providing clear evidence that pronounced local connectivity changes, such as quadrupled increase in WLOCP and heightened BC in shrublands (Figs. 6–9), do not uniformly influence global network properties like GE and LD (Figs. 4 and 5). Despite substantial local alterations, the consistency in global network metrics underscores an inherent resilience within the network's topology, ensuring that overall ecosystem functionality is maintained despite individual patch modifications. This resilience supports the notion that grassland and shrubland endmember states, while functionally distinct, are inherently stable, supporting the endmember stability model proposed by Turnbull et al. (2008).

We have shown how network analysis enables deeper interrogation of structure-functioning relations. Specifically, the heightened sensitivity of sediment transport to landscape structure compared to hydrologic connectivity (Fig. 10) illustrates the contrasting controls on these two processes. This finding has important implications for management strategies, as it suggests that interventions aimed at decoupling sediment fluxes from water and nutrient flows could be effective in combating soil loss while maintaining essential resource redistribution in dryland ecosystems.

The application of network analysis in this study not only enriches our understanding of vegetation shifts and ecosystem transformations but also aligns with broader geomorphic studies. Previous studies have demonstrated how geomorphic processes like erosion and sediment deposition are interconnected across landscapes (Cossart and Fressard, 2017; Heckmann et al., 2015; Sarker et al., 2019), similar to our observations in dryland ecosystems where shifts in vegetation notably alter hydrological and sediment transport pathways. For example, just as Sarker et al., (2019) explored how river connectivity impacts sediment dynamics downstream, our findings illustrate how shrub encroachment influences resource redistribution across hillslopes. This influence on resource distribution is particularly evident through our analysis of betweenness centrality (BC) and weighted length of overland flow paths (WLOCOP), which revealed abrupt connectivity shifts in shrublands affecting erosion and sediment deposition during rain events.

These observations underscore the responsiveness of local interactions, such as water flow and sediment movement, in shaping global network properties and enhancing ecosystem resilience. This streamlined approach affirms the importance of network metrics in understanding complex environmental dynamics across varying conditions, bridging findings from river and proglacial systems to dryland ecosystems.

The utility of network science in this research reveals new dimensions of connectivity dynamics that are critical for understanding vegetation shifts and other ecosystem transformations. By providing a flexible framework for quantifying changes in complex pattern-process relations, this methodology enhances our understanding of dryland resilience. Future research could expand network approaches to integrate habitat, hydrologic, and sediment connectivity, offering a more holistic view of the interactions within social-ecological systems.

As climate change and human activities intensify pressures on fragile dryland regions, the insights gained from this study will be instrumental in formulating scale-aware management strategies. By capturing the intricate multi-level reconfigurations accompanying vegetation shifts in arid systems, our network-based approach not only enriches the scientific discourse on ecosystem management but also supports broad applications across diverse environmental contexts, thereby advancing our capacity to sustain dryland resilience amid global changes.

6. Open research

The network analyses presented in this research were conducted using *MATLAB 2023* The MathWorks Inc, 2023, employing its *graph* functions to evaluate both global and local connectivity patterns. The underlying data supporting these analyses are derived from previously published works, specifically Laura Turnbull, Wainwright, Brazier, et al., 2010 and Laura Turnbull & Wainwright, 2019.

To ensure transparency and reproducibility, the MATLAB code used for these analyses, along with the data, is openly available in the following GitHub repository: *https://github.com/shubhamrt/DrylandConnectivityAnalysis*.

CRediT authorship contribution statement

Shubham Tiwari: Writing – review & editing, Writing – original draft, Visualization, Validation, Methodology, Investigation, Formal analysis, Data curation, Conceptualization. **Laura Turnbull:** Writing – review & editing, Supervision, Resources, Project administration, Funding acquisition, Conceptualization. **John Wainwright:** Writing – review & editing, Supervision, Resources, Project administration, Funding acquisition, Conceptualization.

Declaration of competing interest

The authors declare that they have no known competing financial interests or personal relationships that could have appeared to influence the work reported in this paper.

Acknowledgments

This research was supported by the European Union's Horizon 2020 research and innovation programme under the Marie Sklodowska-Curie grant agreement number 859937. We are also grateful for support from the Sevilleta LTER funded by the National Science Foundation under Grant No. 1655499.

Appendix A. Supplementary data

Supplementary data to this article can be found online at https://doi.org/10.1016/j.jhydrol.2025.132896.

Data availability

Data will be made available on request.

References

Abrahams, A.D., Parsons, A.J., 1996. Rill hydraulic on a semiarid hillslope, Souther Arizona. EARTH Surf. Process. LANDFORMS 21, 35–47. https://doi.org/10.1002/(SICI)1096-9837(199601)21:1.

Abrahams, A.D., Parsons, A.J., Wainwright, J., 2003. Disposition of rainwater under creosotebush. Hydrol. Process. 17, 2555–2566. https://doi.org/10.1002/HYP.1272.

Abrahams, A.D., Parsons, A.J., Wainwright, J., 1995. Controls and determination of resistance to overland flow on semiarid hillslopes, Walnut Gulch. J. Soil Water Conserv. 50.

Barrat, A., Barthélemy, M., Pastor-Satorras, R., Vespignani, A., 2004. The architecture of complex weighted networks. Proc. Natl. Acad. Sci. u. s. a. 101, 3747–3752. https://doi.org/10.1073/PNAS.0400087101/ASSET/7970A6FD-0C68-49D2-AB37-938124DCEAFA/ASSETS/GRAPHIC/ZPQ0080439150007.JPEG.

Bestelmeyer, B.T., Duniway, M.C., James, D.K., Burkett, L.M., Havstad, K.M., 2013. A test of critical thresholds and their indicators in a desertification-prone ecosystem: more resilience than we thought. Ecol. Lett. 16, 339–345. https://doi.org/10.1111/ele.12045.

Bestelmeyer, B.T., Ellison, A.M., Fraser, W.R., Gorman, K.B., Holbrook, S.J., Laney, C.M., Ohman, M.D., Peters, D.P.C., Pillsbury, F.C., Rassweiler, A., Schmitt, R.J., Sharma, S., 2011. Analysis of abrupt transitions in ecological systems. Ecosphere 2, art129. https://doi.org/10.1890/es11-00216.1.

Bestelmeyer, B.T., Peters, D.P.C., Archer, S.R., Browning, D.M., Okin, G.S., Schooley, R. L., Webb, N.P., 2018. The Grassland–Shrubland Regime Shift in the Southwestern United States: Misconceptions and Their Implications for Management. Bioscience 68, 678–690. https://doi.org/10.1093/BIOSCI/BIY065.

Boccaletti, S., Latora, V., Moreno, Y., Chavez, M., Hwang, D.U., 2006. Complex networks: Structure and dynamics. Phys. Rep. https://doi.org/10.1016/j.physrep.2005.10.009.

Bodin, Ö., Norberg, J., 2007. A network approach for analyzing spatially structured populations in fragmented landscape. Landsc. Ecol. 22, 31–44. https://doi.org/10.1007/S10980-006-9015-0/METRICS.

Bodin, Ö., Saura, S., 2010. Ranking individual habitat patches as connectivity providers: integrating network analysis and patch removal experiments. Ecol. Modell. 221, 2393–2405. https://doi.org/10.1016/j.ecolmodel.2010.06.017.

Borselli, L., Cassi, P., Torri, D., 2008. Prolegomena to sediment and flow connectivity in the landscape: A GIS and field numerical assessment. CATENA 75, 268–277. https://doi.org/10.1016/J.CATENA.2008.07.006.

Bracken, L.J., Croke, J., 2007. The concept of hydrological connectivity and its contribution to understanding runoff-dominated geomorphic systems. Hydrol. Process. 21, 1749–1763. https://doi.org/10.1002/hyp.6313.

Bracken, L.J., Turnbull, L., Wainwright, J., Bogaart, P., 2015. Sediment connectivity: A framework for understanding sediment transfer at multiple scales. Earth Surf. Process. Landforms 40, 177–188. https://doi.org/10.1002/esp.3635.

Calvo-Cases, A., Arnau-Rosalén, E., Boix-Fayos, C., Estrany, J., Roxo, M.J., Symeonakis, E., 2021. Eco-geomorphological connectivity and coupling interactions at hillslope scale in drylands: Concepts and critical examples. J. Arid Environ. 186, 104418. https://doi.org/10.1016/j.jaridenv.2020.104418.

Cavalli, M., Trevisani, S., Comiti, F., Marchi, L., 2013. Geomorphometric assessment of spatial sediment connectivity in small Alpine catchments. Geomorphology 188, 31–41. https://doi.org/10.1016/J.GEOMORPH.2012.05.007.

Caylor, K.K., Scanlon, T.M., Rodriguez-Iturbe, I., 2009. Ecohydrological optimization of pattern and processes in water-limited ecosystems: a trade-off-based hypothesis. Water Resour. Res. 45. https://doi.org/10.1029/2008WR007230.

Cossart, É., Fressard, M., 2017. Assessment of structural sediment connectivity within catchments: insights from graph theory. Earth Surf. Dyn. 5, 253–268. https://doi.org/10.5194/ESURF-5-253-2017.

Crompton, O., Katul, G., Lapides, D.A., Thompson, S.E., 2023. Bridging structural and functional hydrological connectivity in dryland ecosystems. CATENA 231, 107322. https://doi.org/10.1016/J.CATENA.2023.107322.

Crucitti, P., Latora, V., Marchiori, M., Rapisarda, A., 2003. Efficiency of scale-free networks: error and attack tolerance. Phys. A Stat. Mech. Its Appl. 320, 622–642. https://doi.org/10.1016/S0378-4371(02)01545-5.

Crucitti, P., Latora, V., Porta, S., 2006. Centrality measures in spatial networks of urban streets. Phys. Rev. E - Stat. Nonlinear, Soft Matter Phys. 73, 036125. https://doi.org/10.1103/PHYSREVE.73.036125/FIGURES/3/THUMBNAIL.

Cunliffe, A.M., Puttock, A.K., Turnbull, L., Wainwright, J., Brazier, R.E., 2016. Dryland, calcareous soils store (and lose) significant quantities of near-surface organic carbon. J. Geophys. Res. Earth Surf. 121, 684–702. https://doi.org/10.1002/2015JF003628.

Dickie, J.A., Parsons, A.J., 2012. ECO-GEOMORPHOLOGICAL PROCESSES WITHIN GRASSLANDS, SHRUBLANDS AND BADLANDS IN THE SEMI-ARID KAROO, SOUTH AFRICA. L. Degrad. Dev. 23, 534–547. https://doi.org/10.1002/LDR.2170.

Eichel, J., Corenblit, D., Dikau, R., 2016. Conditions for feedbacks between geomorphic and vegetation dynamics on lateral moraine slopes: a biogeomorphic feedback window. Earth Surf. Process. Landforms 41, 406–419. https://doi.org/10.1002/ESP.3859.

Eichel, J., Draebing, D., Winkler, S., Meyer, N., 2023. Similar vegetation-geomorphic disturbance feedbacks shape unstable glacier forelands across mountain regions. Ecosphere 14, e4404.

Folke, C., 2006. Resilience: The emergence of a perspective for social–ecological systems analyses. Glob. Environ. Chang. 16, 253–267. https://doi.org/10.1016/j.gloenvcha.2006.04.002.

Freeman, L.C., 1978. Centrality in social networks conceptual clarification. Soc. Networks 1, 215–239.

Gao, Q., Reynolds, J.F., 2003. Historical shrub-grass transitions in the northern Chihuahuan Desert: modeling the effects of shifting rainfall seasonality and event size over a landscape gradient. Glob. Chang. Biol. 9, 1475–1493. https://doi.org/10.1046/j.1365-2486.2003.00676.x.

Girvan, M., Newman, M.E.J., 2002. Community structure in social and biological networks. Proc. Natl. Acad. Sci. 99, 7821–7826. https://doi.org/10.1073/pnas.122653799.

Harel, M.A., Mouche, E., 2014. Is the connectivity function a good indicator of soil infiltrability distribution and runoff flow dimension? Earth Surf. Process. Landforms 39, 1514–1525. https://doi.org/10.1002/esp.3604.

Heckmann, T., Schwanghart, W., 2013. Geomorphic coupling and sediment connectivity in an alpine catchment — Exploring sediment cascades using graph theory. Geomorphology 182, 89–103. https://doi.org/10.1016/j.geomorph.2012.10.033.

Heckmann, T., Schwanghart, W., Phillips, J.D., 2015. Graph theory—Recent developments of its application in geomorphology. Geomorphology 243, 130–146. https://doi.org/10.1016/J.GEOMORPH.2014.12.024.

Hervías-Parejo, S., Tur, C., Heleno, R., Nogales, M., Timóteo, S., Traveset, A., 2020. Species functional traits and abundance as drivers of multiplex ecological networks: first empirical quantification of inter-layer edge weights. Proc. r. Soc. B Biol. Sci. 287, 20202127. https://doi.org/10.1098/rspb.2020.2127.

Hiatt, M., Addink, E.A., Kleinhans, M.G., 2022. Connectivity and directionality in estuarine channel networks. Earth Surf. Process. Landforms 47, 807–824. https://doi.org/10.1002/esp.5286.

Hiatt, M., Castañeda-Moya, E., Twilley, R., Hodges, B.R., Passalacqua, P., 2018. Channel-island connectivity affects water exposure time distributions in a coastal river delta. Water Resour. Res. 54, 2212–2232. https://doi.org/10.1002/2017WR021289.

Holling, C.S., 1973. Resilience and Stability of Ecological Systems. Annu. Rev. Ecol. Evol. Syst. 4, 1–23. https://doi.org/10.1146/ANNUREV.ES.04.110173.000245.

Jacquet, C., Carraro, L., Altermatt, F., 2022. Meta-ecosystem dynamics drive the spatial distribution of functional groups in river networks. Oikos 2022, e09372. https://doi.org/10.1111/oik.09372.

James, J.J., Sheley, R.L., Erickson, T., Rollins, K.S., Taylor, M.H., Dixon, K.W., 2013. A systems approach to restoring degraded drylands. J. Appl. Ecol. 50, 730–739. https://doi.org/10.1111/1365-2664.12090.

Jenerette, G.D., Barron-Gafford, G.A., Guswa, A.J., McDonnell, J.J., Villegas, J.C., 2012. Organization of complexity in water limited ecohydrology. Ecohydrology 5, 184–199. https://doi.org/10.1002/eco.217.

Kéfi, S., Couteron, P., 2018. Spatiotemporal patterns as indicators of approaching critical transitions. Ecol. Indic. https://doi.org/10.1016/j.ecolind.2018.07.034.

King, E.G., Franz, T.E., Caylor, K.K., 2012. Ecohydrological interactions in a degraded two-phase mosaic dryland: implications for regime shifts, resilience, and restoration. Ecohydrology 5, 733–745. https://doi.org/10.1002/eco.260.

Kleineberg, K.K., Boguñá, M., Ángeles Serrano, M., Papadopoulos, F., 2016. Hidden geometric correlations in real multiplex networks. Nat. Phys. 12, 1076–1081. https://doi.org/10.1038/nphys3812.

Krause, A.E., Frank, K.A., Mason, D.M., Ulanowicz, R.E., Taylor, W.W., 2003. Compartments revealed in food-web structure. Nat. 2003 4266964 426, 282–285. 10.1038/nature02115.

Lal, R., 2019. Carbon cycling in global drylands. Curr. Clim. Chang. Reports. 10.1007/s40641-019-00132-z.

Latora, V., Marchiori, M., 2001. Efficient Behavior of Small-World Networks. PhysRevLett 87, 198701. https://doi.org/10.1103/PhysRevLett.87.198701.

Liégeois, R., Santos, A., Matta, V., Van De Ville, D., Sayed, A.H., 2020. Revisiting correlation-based functional connectivity and its relationship with structural connectivity. Netw. Neurosci. 4, 1235–1251. https://doi.org/10.1162/NETN_A_00166.

Maestre, F.T., Benito, B.M., Berdugo, M., Concostrina-Zubiri, L., Delgado-Baquerizo, M., Eldridge, D.J., Guirado, E., Gross, N., Kéfi, S., Le Bagousse-Pinguet, Y., Ochoa-Hueso, R., Soliveres, S., 2021. Biogeography of global drylands. New Phytol. 231, 540–558. https://doi.org/10.1111/nph.17395.

Maestre, F.T., Eldridge, D.J., Soliveres, S., Kéfi, S., Delgado-Baquerizo, M., Bowker, M.A., García-Palacios, P., Gaitán, J., Gallardo, A., Lázaro, R., Berdugo, M., 2016a. Structure and functioning of dryland ecosystems in a changing world. Annu. Rev. Ecol. Evol. Syst. 47, 215–237. https://doi.org/10.1146/annurev-ecolsys-121415-032311.

Maestre, F.T., Eldridge, D.J., Soliveres, S., Kéfi, S., Delgado-Baquerizo, M., Bowker, M.A., García-Palacios, P., Gaitán, J., Gallardo, A., Lázaro, R., Berdugo, M., 2016b. Structure and functioning of dryland ecosystems in a changing world. https://doi.org/10.1146/annurev-ecolsys-121415-032311 47, 215–237. 10.1146/ANNUREV-ECOLSYS-121415-032311.

Maestre, F.T., Le Bagousse-Pinguet, Y., Delgado-Baquerizo, M., Eldridge, D.J., Saiz, H., Berdugo, M., Gozalo, B., Ochoa, V., Guirado, E., García-Gómez, M., Valencia, E., Gaitán, J.J., Asensio, S., Mendoza, B.J., Plaza, C., Díaz-Martínez, P., Rey, A., Hu, H.-W., He, J.-Z., Wang, J.-T., Lehmann, A., Rillig, M.C., Cesarz, S., Eisenhauer, N., Martínez-Valderrama, J., Moreno-Jiménez, E., Sala, O., Abedi, M., Ahmadian, N., Alados, C.L., Aramayo, V., Amghar, F., Arredondo, T., Ahumada, R.J., Bahalkeh, K., Ben Salem, F., Blaum, N., Boldgiv, B., Bowker, M.A., Bran, D., Bu, C., Canessa, R., Castillo-Monroy, A.P., Castro, H., Castro, I., Castro-Quezada, P., Chibani, R., Conceição, A.A., Currier, C.M., Darrouzet-Nardi, A., Deák, B., Donoso, D.A., Dougill, A.J., Durán, J., Erdenetsetseg, B., Espinosa, C.I., Fajardo, A., Farzam, M., Ferrante, D., Frank, A.S.K., Fraser, L.H., Gherardi, L.A., Greenville, A.C., Guerra, C. A., Gusmán-Montalvan, E., Hernández-Hernández, R.M., Hölzel, N., Huber-Sannwald, E., Hughes, F.M., Jadán-Maza, O., Jeltsch, F., Jentsch, A., Kaseke, K.F., Köbel, M., Koopman, J.E., Leder, C.V., Linstädter, A., le Roux, P.C., Li, X., Liancourt, P., Liu, J., Louw, M.A., Maggs-Kölling, G., Makhalanyane, T.P., Issa, O.M., Manzaneda, A.J., Marais, E., Mora, J.P., Moreno, G., Munson, S.M., Nunes, A., Oliva, G., Oñatibia, G.R., Peter, G., Pivari, M.O.D., Pueyo, Y., Quiroga, R.E., Rahmanian, S., Reed, S.C., Rey, P.J., Richard, B., Rodríguez, A., Rolo, V.,

Rubalcaba, J.G., Ruppert, J.C., Salah, A., Schuchardt, M.A., Spann, S., Stavi, I., Stephens, C.R.A., Swemmer, A.M., Teixido, A.L., Thomas, A.D., Throop, H.L., Tielbörger, K., Travers, S., Val, J., Valkó, O., van den Brink, L., Ayuso, S.V., Velbert, F., Wamiti, W., Wang, D., Wang, L., Wardle, G.M., Yahdjian, L., Zaady, E., Zhang, Y., Zhou, X., Singh, B.K., Gross, N., 2022. Grazing and ecosystem service delivery in global drylands. Science (80-) 378, 915–920. https://doi.org/10.1126/science.abq4062.
Mayor, A., Bautista, S., Rodriguez, F., Kéfi, S., 2019. Connectivity-mediated ecohydrological feedbacks and regime shifts in drylands. Ecosystems 22, 1497–1511. https://doi.org/10.1007/s10021-019-00366-w.
Mayor, A., Kéfi, S., Bautista, S., Rodríguez, F., Cartení, F., Rietkerk, M., 2013. Feedbacks between vegetation pattern and resource loss dramatically decrease ecosystem resilience and restoration potential in a simple dryland model. Landsc. Ecol. 28, 931–942. https://doi.org/10.1007/s10980-013-9870-4.
Meron, E., 2018. From Patterns to Function in Living Systems: Dryland Ecosystems as a Case Study. 10.1146/annurev-conmatphys-033117-053959 9, 79–103. 10.1146/ANNUREV-CONMATPHYS-033117-053959.
Mueller, E.N., Tietjen, B., Turnbull, L., Wainwright, J., 2014. Ecohydrological modelling of land degradation in drylands: feedbacks between water, erosion, vegetation and soil.
Newman, M.E.J., 2006. Modularity and community structure in networks. Proc. Natl. Acad. Sci. u. s. a. 103, 8577–8582. https://doi.org/10.1073/PNAS.0601602103/ASSET/F86312F7-1DFE-4A0E-928F-6C1D4161BF34/ASSETS/GRAPHIC/ZPQ02306-2388-M07.JPEG.
Newman, M.E.J., 2002. Assortative mixing in networks. Phys. Rev. Lett. 89, 208701. https://doi.org/10.1103/PHYSREVLETT.89.208701/FIGURES/1/MEDIUM.
Nichols, M.H., Magirl, C., Sayre, N.F., Shaw, J.R., 2018. The geomorphic legacy of water and erosion control structures in a semiarid rangeland watershed. Earth Surf. Process. Landforms 43, 909–918. https://doi.org/10.1002/ESP.4287.
Noy-Meir, I., 1973. Desert ecosystems: environment and producers. Annu. Rev. Ecol. Syst. 4, 25–51. https://doi.org/10.1146/annurev.es.04.110173.000325.
Okin, G.S., De Las Heras, M.M., Saco, P.M., Throop, H.L., Vivoni, E.R., Parsons, A.J., Wainwright, J., Peters, D.P.C., 2015. Connectivity in dryland landscapes: Shifting concepts of spatial interactions. Front. Ecol. Environ. https://doi.org/10.1890/140163.
Okin, G.S., Parsons, A.J., Wainwright, J., Herrick, J.E., Bestelmeyer, B.T., Peters, D.C., Fredrickson, E.L., 2009. Do changes in connectivity explain desertification? Bioscience 59, 237–244. https://doi.org/10.1525/bio.2009.59.3.8.
Parsons, A.J., Abrahams, A.D., Wainwright, J., 1996. Responses of interrill runoff and erosion rates to vegetation change in southern Arizona. Geomorphology 14, 311–317. https://doi.org/10.1016/0169-555X(95)00044-6.
Parsons, A.J., Abrahams, A.D., Wainwright, J., 1994. Rainsplash and erosion rates in an interrill area on semi-arid grassland, Southern Arizona. CATENA 22, 215–226. https://doi.org/10.1016/0341-8162(94)90003-5.
Passalacqua, P., 2017. The Delta Connectome: A network-based framework for studying connectivity in river deltas. Geomorphology 277, 50–62. https://doi.org/10.1016/j.geomorph.2016.04.001.
Peters, D.P.C., Bestelmeyer, B.T., Herrick, J.E., Fredrickson, E.L., Monger, H.C., Havstad, K.M., 2006. Disentangling complex landscapes: New insights into arid and semiarid system dynamics. Bioscience 56, 491–501. https://doi.org/10.1641/0006-3568(2006)56[491:DCLNII]2.0.CO;2.
Peters, D.P.C., Okin, G.S., Herrick, J.E., Savoy, H.M., Anderson, J.P., Scroggs, S.L., Zhang, J., 2020. Modifying connectivity to promote state change reversal: the importance of geomorphic context and plant–soil feedbacks. Ecology. https://doi.org/10.1002/ecy.3069.
Pierce, N.A., Archer, S.R., Bestelmeyer, B.T., James, D.K., 2019. Grass-shrub competition in arid lands: an overlooked driver in grassland–shrubland state transition? Ecosystems 22, 619–628. https://doi.org/10.1007/s10021-018-0290-9.
Pilosof, S., Porter, M.A., Pascual, M., Kéfi, S., 2017. The multilayer nature of ecological networks. Nat. Ecol. Evol. 10.1038/s41559-017-0101.
Prăvălie, R., 2016. Drylands extent and environmental issues: A global approach. Earth-Science Rev. 161, 259–278. https://doi.org/10.1016/j.earscirev.2016.08.003.
Price, M.F., 2003. Panarchy: Understanding Transformations in Human and Natural Systems: Edited by Lance H. Gunderson and C.S. Holling. Island Press, 2002. xxiv+507 pages. ISBN 1-55963-857-5 (paper), $35. Biol. Conserv. 114, 308–309. 10.1016/S0006-3207(03)00041-7.
Reynolds, J.F., Stafford Smith, D.M., Lambin, E.F., Turner, B.L., Mortimore, M., Batterbury, S.P.J., Downing, T.E., Dowlatabadi, H., Fernández, R.J., Herrick, J.E., Huber-Sannwald, E., Jiang, H., Leemans, R., Lynam, T., Maestre, F.T., Ayarza, M., Walker, B., 2007. Ecology: Global desertification: Building a science for dryland development. Science (80-.). 10.1126/science.1131634.
Romero Ovalle, P.E., Bisigato, A.J., Campanella, M.V., 2021. Soil erosion facilitates shrub encroachment in Patagonian herbaceous steppes. L. Degrad. Dev. 32, 3377–3385. https://doi.org/10.1002/ldr.4016.
Saco, P.M., Rodríguez, J.F., Moreno-de las Heras, M., Keesstra, S., Azadi, S., Sandi, S., Baartman, J., Rodrigo-Comino, J., Rossi, M.J., 2020. Using hydrological connectivity to detect transitions and degradation thresholds: Applications to dryland systems. CATENA 186, 104354. https://doi.org/10.1016/j.catena.2019.104354.
Sarker, S., Veremyev, A., Boginski, V., Singh, A., 2019. Critical Nodes in river networks. Sci. Rep. 9. https://doi.org/10.1038/s41598-019-47292-4.
Scheffer, M., Carpenter, S.R., 2003. Catastrophic regime shifts in ecosystems: linking theory to observation. Trends Ecol. Evol. https://doi.org/10.1016/j.tree.2003.09.002.
Schlesinger, W.H., Reynolds, J.F., Cunningham, G.L., Huenneke, L.F., Jarrell, W.M., Virginia, R.A., Whitford, W.G., 1990. Biological feedbacks in global desertification. Science (80-) 247, 1043–1048. https://doi.org/10.1126/science.247.4946.1043.
Stauffer, D., Aharony, A., 2018. Introduction To Percolation Theory : Second Edition. Introd. To Percolation Theory. 10.1201/9781315274386.
Stewart, J., Parsons, A.J., Wainwright, J., Okin, G.S., Bestelmeyer, B.T., Fredrickson, E.L., Schlesinger, W.H., 2014. Modeling emergent patterns of dynamic desert ecosystems. Ecol. Monogr. 84, 373–410. https://doi.org/10.1890/12-1253.1.
Tejedor, A., Longjas, A., Zaliapin, I., Foufoula-Georgiou, E., 2015. Delta channel networks: 1. A graph-theoretic approach for studying connectivity and steady state transport on deltaic surfaces. Water Resour. Res. 51, 3998–4018. https://doi.org/10.1002/2014WR016577.
The MathWorks Inc. MATLAB, 2023.
Thompson, S.E., Assouline, S., Chen, L., Trahktenbrot, A., Svoray, T., Katul, G.G., 2014. Secondary dispersal driven by overland flow in drylands: Review and mechanistic model development. Mov. Ecol. 2, 7. https://doi.org/10.1186/2051-3933-2-7.
Tiwari, S., Brizuela, S.R., Hein, T., Turnbull, L., Wainwright, J., Funk, A., 2024. Water-controlled ecosystems as complex networks: Evaluation of network-based approaches to quantify patterns of connectivity. Ecohydrology N/a e2690. https://doi.org/10.1002/eco.2690.
Tiwari, S., Jha, S.K., Singh, A., 2020. Quantification of node importance in rain gauge network: influence of temporal resolution and rain gauge density. Sci. Rep. 10. https://doi.org/10.1038/s41598-020-66363-5.
Turnbull, L., Hütt, M.-T., Ioannides, A.A., Kininmonth, S., Poeppl, R., Tockner, K., Bracken, L.J., Keesstra, S., Liu, L., Masselink, R., Parsons, A.J., 2018. Connectivity and complex systems: learning from a multi-disciplinary perspective. Appl. Netw. Sci. 3, 11. https://doi.org/10.1007/s41109-018-0067-2.
Turnbull, L., Wainwright, J., 2019. From structure to function: Understanding shrub encroachment in drylands using hydrological and sediment connectivity. Ecol. Indic. 98, 608–618. https://doi.org/10.1016/j.ecolind.2018.11.039.
Turnbull, L., Wainwright, J., Brazier, R.E., 2010a. Hydrology, erosion and nutrient transfers over a transition from semi-arid grassland to shrubland in the South-Western USA: A modelling assessment. J. Hydrol. 388, 258–272. https://doi.org/10.1016/J.JHYDROL.2010.05.005.
Turnbull, L., Wainwright, J., Brazier, R.E., 2010b. Changes in hydrology and erosion over a transition from grassland to shrubland. Hydrol. Process. 24, 393–414. https://doi.org/10.1002/HYP.7491.
Turnbull, L., Wainwright, J., Brazier, R.E., 2008. A conceptual framework for understanding semi-arid land degradation: ecohydrological interactions across multiple-space and time scales. Ecohydrology 1, 23–34. https://doi.org/10.1002/eco.4.
Turnbull, L., Wainwright, J., Brazier, R.E., Bol, R., 2010c. Biotic and Abiotic Changes in Ecosystem Structure over a Shrub-Encroachment Gradient in the Southwestern USA. Ecosystems 13, 1239–1255. https://doi.org/10.1007/s10021-010-9384-8.
Turnbull, L., Wilcox, B.P., Belnap, J., Ravi, S., D'Odorico, P., Childers, D., Gwenzi, W., Okin, G., Wainwright, J., Caylor, K.K., Sankey, T., 2012. Understanding the role of ecohydrological feedbacks in ecosystem state change in drylands. Ecohydrology 5, 174–183. https://doi.org/10.1002/eco.265.
United Nations., 2022. The Global Land Outlook, second edition.
Van Auken, O.W., 2000. Shrub invasions of North American semiarid grasslands. Annu. Rev. Ecol. Syst. 31, 197–215. https://doi.org/10.1146/annurev.ecolsys.31.1.197.
Ventresca, M., Aleman, D., 2015. Efficiently identifying critical nodes in large complex networks. Comput. Soc. Networks 2015 21 2, 1–16. 10.1186/S40649-015-0010-Y.
Veremyev, A., Prokopyev, O.A., Pasiliao, E.L., 2015. Critical nodes for distance-based connectivity and related problems in graphs. Networks 66, 170–195. https://doi.org/10.1002/net.21622.
Voutsa, V., Battaglia, D., Bracken, L., Brovelli, A., Costescu, J., Muñoz, M., Fath, B., Funk, A., Guirro, M., Hein, T., Kerschner, C., Kimmich, C., Lima, V., Messé, A., Parsons, A., Perez, J., Pöppl, R., Prell, C., Recinos, S., Shi, Y., Tiwari, S., Turnbull, L., Wainwright, J., Waxenecker, H., Hütt, M., 2021. Two classes of functional connectivity in dynamical processes in networks. J. R. Soc. Interface 18. https://doi.org/10.1098/RSIF.2021.0486.
Wainwright, J., Parsons, A., Schlesinger, W., Abrahams, A., 2002. Hydrology-vegetation interactions in areas of discontinuous flow on a semi-arid bajada, Southern New Mexico. J. Arid Environ. 51, 319–338. https://doi.org/10.1006/jare.2002.0970.
Wainwright, J., Parsons, A.J., Müller, E.N., Brazier, R.E., Powell, D.M., Fenti, B., 2008a. A transport-distance approach to scaling erosion rates: 1. Background and model development. Earth Surf. Process. Landforms 33, 813–826. https://doi.org/10.1002/esp.1624.
Wainwright, J., Parsons, A.J., Müller, E.N., Brazier, R.E., Powell, D.M., Fenti, B., 2008b. A transport-distance approach to scaling erosion rates: 2. sensitivity and evaluation of Mahleran. Earth Surf. Process. Landforms 33, 962–984. https://doi.org/10.1002/esp.1623.
Wainwright, J., Parsons, A.J., Müller, E.N., Brazier, R.E., Powell, D.M., Fenti, B., 2008c. A transport-distance approach to scaling erosion rates: 3. Evaluating scaling characteristics ofMahleran. Earth Surf. Process. Landforms 33, 1113–1128. https://doi.org/10.1002/esp.1622.

Wainwright, J., Turnbull, L., Ibrahim, T.G., Lexartza-Artza, I., Thornton, S.F., Brazier, R. E., 2011. Linking environmental régimes, space and time: Interpretations of structural and functional connectivity. Geomorphology 126, 387–404. https://doi.org/10.1016/j.geomorph.2010.07.027.

Wilcox, B.P., Basant, S., Olariu, H., Leite, P.A.M., 2022. Ecohydrological connectivity: A unifying framework for understanding how woody plant encroachment alters the water cycle in drylands. Front. Environ. Sci. 10, 1779. https://doi.org/10.3389/FENVS.2022.934535/BIBTEX.

Wohl, E., Brierley, G., Cadol, D., Coulthard, T.J., Covino, T., Fryirs, K.A., Grant, G., Hilton, R.G., Lane, S.N., Magilligan, F.J., Meitzen, K.M., Passalacqua, P., Poeppl, R. E., Rathburn, S.L., Sklar, L.S., 2019. Connectivity as an emergent property of geomorphic systems. Earth Surf. Process. Landforms 44, 4–26. https://doi.org/10.1002/esp.4434.

Zhang, Y., Ng, S.T., 2021. Identification and quantification of node criticality through EWM–TOPSIS: A Study of Hong Kong's MTR System. Urban Rail Transit 2021 73 7, 226–239. 10.1007/S40864-021-00155-6.